Molecular Biology of the Cell
Vol. 12, 901–917, April 2001

The *Schizosaccharomyces pombe spo20*$^+$ Gene Encoding a Homologue of *Saccharomyces cerevisiae* Sec14 Plays an Important Role in Forespore Membrane Formation

Yukiko Nakase,* Taro Nakamura,* Aiko Hirata,† Sheri M. Routt,‡ Henry B. Skinner,‡ Vytas A. Bankaitis,‡ and Chikashi Shimoda*§

*Department of Biology, Graduate School of Science, Osaka City University, Sumiyoshi-ku, Osaka 558-8585, Japan; †Institute of Molecular and Cellular Biosciences, The University of Tokyo, Bunkyo-ku, Tokyo 113-0032; and ‡Department of Cell Biology, University of Alabama at Birmingham, Birmingham, Alabama 35294-0005

Submitted July 11, 2000; Revised January 2, 2001; Accepted February 5, 2001
Monitoring Editor: Chris Kaiser

The *Schizosaccharomyces pombe spo20-KC104* mutation was originally isolated in a screen for sporulation-deficient mutants, and the *spo20-KC104* mutant exhibits temperature-sensitive growth. Herein, we report that *S. pombe*, *spo20*$^+$ is essential for fission yeast cell viability and is constitutively expressed throughout the life cycle. We also demonstrate that the *spo20*$^+$ gene product is structurally homologous to *Saccharomyces cerevisiae* Sec14, the major phosphatidylinositol transfer protein of budding yeast. This structural homology translates to a significant degree of functional relatedness because reciprocal complementation experiments demonstrate that each protein is able to fulfill the essential function of the other. Moreover, biochemical experiments show that, like Sec14, Spo20 is a phosphatidylinositol/phosphatidylcholine-transfer protein. That Spo20 is required for Golgi secretory function in vegetative cells is indicated by our demonstration that the *spo20-KC104* mutant accumulates aberrant Golgi cisternae at restrictive temperatures. However, a second phenotype observed in Spo20-deficient fission yeast is arrest of cell division before completion of cell separation. Consistent with a direct role for Spo20 in controlling cell septation in vegetatively growing cells, localization experiments reveal that Spo20 preferentially localizes to the cell poles and to sites of septation of fission yeast cells. We also report that, when fission yeasts are challenged with nitrogen starvation, Spo20 translocates to the nucleus. This nuclear localization persists during conjugation and meiosis. On completion of meiosis, Spo20 translocates to forespore membranes, and it is the assembly of forespore membranes that is abnormal in *spo20-KC104* cells. In such mutants, a considerable fraction of forming prespores fail to encapsulate the haploid nucleus. Our results indicate that Spo20 regulates the formation of specialized membrane structures in addition to its recognized role in regulating Golgi secretory function.

INTRODUCTION

Sporulation in the fission yeast *Schizosaccharomyces pombe* exhibits analogies with gametogenesis in higher eukaryotes. *S. pombe* cells initiate a sporulation program when challenged with nutrient starvation, particularly when nitrogen is the limiting nutrient (Egel, 1971, 1989; Yamamoto *et al.*, 1997). Sporulation represents a culmination of two meiotic divisions that generate four haploid nuclei which are packaged into individual spores (Egel, 1971, 1989; Yamamoto *et al.*, 1997). Spore formation requires assembly of double-layered intracellular membranes, termed forespore membranes (Yoo *et al.*, 1973), which is equivalent to the prospore wall in *Saccharomyces cerevisiae* (Byers, 1981). During meiosis II, forespore membranes are assembled by the fusion of membrane vesicles (Hirata and Tanaka, 1982; Tanaka and Hirata, 1982). From metaphase II to anaphase II, the spindle pole body (SPB), which plays a crucial role in spindle microtubule formation, undergoes a morphological transfor-

§ Corresponding author. E-mail address: shimoda@sci.osaka-cu.ac.jp.

mation into a multilayered structure. Membrane vesicles are then recruited to the vicinity of modified SPBs and subsequently fuse there to generate forespore membranes (Hirata and Tanaka, 1982; Tanaka and Hirata, 1982). As the nucleus divides in meiosis II, the forespore membrane extends, and eventually encapsulates, each of the four nuclei. Herein, we define this membrane-bounded precursor of the spore as the prespore. Finally, the inner layer of the forespore membrane becomes the spore plasma membrane. In the space between the inner and outer prespore membranes, spore wall materials are deposited to form two layers of spore walls (Yoo *et al.*, 1973; Tanaka and Hirata, 1982). Mature spores are then liberated from an ascus when ascus walls are autolyzed (Tanaka and Hirata, 1982).

Many sporulation-deficient *S. pombe* mutants have been isolated (Bresch *et al.*, 1968, Kishida and Shimoda, 1986). Cytological studies classify these mutants into three groups. Class I *spo*$^+$ gene products are involved in structural modification of SPBs. A representative class I gene, *spo15*$^+$, encodes a coiled-coil SPB protein that is essential for the SPB modification (Ikemoto *et al.*, 2000). Class II *spo*$^-$ mutants fail to assemble fully extended forespore membranes, although their SPBs are appropriately modified. The *spo14-B221* mutant is a representative of this class, and it exhibits a cold-sensitive sporulation defect (Kishida *et al.*, 1990). Assembly of forespore membranes is incomplete at restrictive temperatures in *spo14-B221* mutants (Kubo, Nakamura, and Shimoda, unpublished data). Class III *spo*$^-$ mutants form spore-like bodies that are bounded by spore walls but do not contain the nucleus (Hirata and Shimoda, 1992). The class III *spo*$^+$ gene products likely play important roles in spatial and temporal coordination between spore envelope formation and meiotic nuclear division.

Forespore membranes are assembled by fusion of small vesicles. The mechanisms, by which such vesicles are formed, gathered, and fused, are not well understood. Neiman (1998) reported that late-acting secretory genes, such as *SEC1*, *SEC4*, and *SEC8*, are required for forespore membrane formation in the budding yeast *S. cerevisiae*. These cumulative findings establish that both general and sporulation-specific components of the secretory pathway are involved in spore morphogenesis.

So far, class III *spo*$^-$ mutants have not been studied. In this report, we describe the characterization of the *spo20*$^+$ gene product and the phenotypes of *spo20* mutants. Spo20 is structurally and functionally related to the major *S. cerevisiae* phosphatidylinositol (PtdIns)/phosphatidylcholine (PtdCho)-transfer protein Sec14. We demonstrate that Spo20 not only functions to stimulate Golgi secretory function in fission yeast, but is required for completion of cytokinesis in vegetative cells. Finally, we establish that Spo20 localizes to forespore membranes in sporulating cells and that forespore membrane formation around haploid nuclei is abnormal in *spo20* mutants. These findings document a novel function for Sec14-like PtdIns-/PtdCho-transfer proteins (PITPs) in coordinating spore membrane biogenesis with meiotic nuclear division.

MATERIALS AND METHODS

Yeast Strains, Media, and Culture Conditions

S. pombe strains used in this study are listed in Table 1. A sporulation-deficient mutant of *S. pombe*, *spo20-KC104*, was isolated and analyzed by Kishida and Shimoda (1986). The complete medium YEA supplemented with 75 μg/ml adenine sulfate and 50 μg/ml uracil was used for growth. Malt extract medium MEA and synthetic sporulation medium SSL-N and MM-N were used for mating and sporulation. These media were described by Egel and Egel-Mitani (1974), Gutz *et al.* (1974), and Moreno *et al.* (1990). *S. pombe* cells were grown at 30°C and sporulated at 28°C except for the *spo20* mutant, which was grown and sporulated at 25°C. Yeast peptone dextrose medium, defined minimal media, and procedures for transformation of *S. cerevisiae* with plasmid DNA in the presence of lithium acetate have been described (Ito *et al.*, 1983; Sherman *et al.*, 1983). *S. cerevisiae* strains used in this study are also listed in Table 1. YEplac195 is a multicopy plasmid that bears *URA3* for selection in *S. cerevisiae*, and this plasmid served as the vector for the expression constructs used herein.

Cloning of spo20$^+$

A homothallic *spo20* mutant (YN8) was transformed with an *S. pombe* genomic library, pTN-F2, containing partial *Sau3A*I fragments constructed in a multicopy plasmid pFL20 (Losson and Lacroute, 1983), and with a cDNA library, pTN-RC5, containing meiotic cDNA fragments constructed in the expression vector pREP42 (Maundrell, 1993). Two of 15,000 transformants from the genomic library and one of 10,000 transformants from the cDNA library were able to grow at 37°C. All three Ts$^+$ transformants also regained the ability to sporulate. Plasmid DNAs were recovered from these transformants, and two plasmids obtained from the genomic library were analyzed further.

Plasmid Construction

Plasmid pAL(*spo20*)-HA was constructed as follows. A 1.8-kb *Not*I–*Sac*I fragment of pSLF273 (Forsburg and Sherman, 1997), which contains the influenza hemagglutinin (HA) epitope and the *nmt1* terminator, was ligated into the corresponding sites of pAL-KS (Tanaka *et al.*, 2000) to create pTN144. The *spo20* gene was then amplified by PCR using 5′-CCCCTCGAG(*Xho*I)TGCTTCCTGCCTTTAGTAAC-3′ and 5′-CCCGCGGCCGC(*Not*I)AATTTTTGTTCATCCACTG-3′ as forward and reverse primers. The PCR product was digested with *Xho*I and *Not*I and then ligated into the corresponding sites of pTN144, yielding pAL(spo20)-HA.

Plasmid pIU(Δ5′-*spo20*)-HA was constructed as follows. A 1.8-kb *Ssp*I–*Ssp*I fragment containing *ura4*$^+$ was ligated into the corresponding site of Bluescript KS$^-$ to create pIU. A 1.8-kb *Not*I–*Sac*I fragment, which contains the HA epitope and the *nmt1* terminator of pSLF273 (Forsburg and Sherman, 1997), was then ligated into the corresponding sites of pIU to create pIU-HA. The *spo20* gene was then amplified by PCR using 5′-CCCAAGCTT(*Hin*dIII)ATGTCAGAAACTATATCGG-3′ and 5′CCCGCGGCCGC(*Not*I)AATTTTTGTTCATCCACTG-3′ as primers. The PCR product was digested with *Hin*dIII and *Not*I and then ligated into the same sites of pIU-HA, yielding pIU(Δ5′-*spo20*)-HA.

Plasmid pAL(*spo20*^{G275D})-HA was constructed by PCR amplification of the *spo20* ^{G275D} gene using 5′-CCCCTCGAG(*Xho*I)TGCTTCCTGCCTTTAGTAAC-3′ and 5′-CCCGCGGCCGC(*Not*I)AATTTTTGTTCATCCACTG-3′ as primers. The PCR product was digested with *Xho*I and *Not*I and then ligated into the corresponding sites of pTN144, yielding pAL(*spo20*^{G275D})-HA.

Plasmid pIU(Δ5′-*spo20* ^{G275D})-HA was constructed by PCR-amplifying *spo20*^{G275D} using 5′-CCCAAGCTT(*Hin*dIII)ATGTCAGAAACTATATCGG-3′ and 5′-CCCGCGGCCGC(*Not*I)AATTTTTGTTCATCCACTG-3′ as primers. The PCR product was digested with *Hin*dIII and *Not*I and then ligated into the corresponding sites of pIU-HA, yielding pIU(Δ5′-*spo20*^{G275D})-HA.

Plasmid pREP1*spo20* was constructed as follows. Two oligonucleotides were used to amplify the *spo20* gene by PCR using 5′-CCCGTCGAC(*Sal*I)AATGTCAGAAACTATATCGG-3′ and 5′-CAAAATCGTAATATGCAGCTTGAATGGGC-3′ as primers. The

Table 1. *Schizosaccharomyces pombe* and *Saccharomyces cerevisiae* strains used in this study

Strain	Genotype	Source
S. pombe		
YN8	*h*^{90} *spo20-KC104 ura4-D18*	This study
YN8-WH	*h*^{90} *ura4-D18 spo20-HA≪ura4*$^{+}$	This study
YN8-MH	*h*^{90} *ura4-D18 spo20* ^{G275D}*-HA≪ura4*$^{+}$	This study
YN9	*h*^{90} *spo20-KC104 ura4-D18 leu1-32*	This study
YN9-WH	*h*^{90} *ura4-D18 leu1-32 spo20-HA≪ura4*$^{+}$	This study
YN10	*h*^{90} *spo20-KC104*	This study
YN11	*h*^{90} *spo20-KC104 leu1-32*	This study
YN12	*h*^{90}	This study
YN13	*h*$^{+S}$ *spo20-KC104 ade6-M210*	This study
YN14	*h*$^{-}$ *spo20-KC104 ade6-M216*	This study
YN15	*h*^{90}*/h*^{90} *ade6-M210/ade6-M216 leu1/leu1 ura4-D18/ura4-D18*	This study
YN16	*h*^{90}*/h*^{90} *ade6-M210/ade6-M216 leu1/leu1 ura4-D18/ura4-D18 spo20*$^{+}$*/spo20::ura4*$^{+}$	This study
YN13-14	*h*$^{+S}$*/h*$^{-}$ *spo20-KC104/spo20-KC104 ade6-M210/ade6-M216*	This study
YN47-53	*h*$^{+S}$*/h*$^{-}$ *ade6-M210/ade6-M216*	This study
TN9	*h*^{90} *ura4-D18*	This study
TN29	*h*^{90} *ura4-D18 leu1-32*	S. Ikemoto
TN47	*h*$^{+S}$ *ade6-M216*	This study
TN53	*h*$^{-}$ *ade6-M210*	This study
C766-1A	*h*^{90} *leu1-32*	This study
SI53	*h*^{90}	S. Ikemoto
L968	*h*^{90}	U. Leupold
S. cerevisiae		
CTY69	*MATα ade2-101 ura3-52 his3Δ200 trp1Δ sec14-1*	K. Takegawa
CTY303	*MATa ura3-52 his3Δ200 cki1-1 sec14Δ::hisG*	V.A. Bankaitis
CTY808	*MATa ura3-52 his3Δ200 cki1-1 sec14Δ::hisG YEplac195*	V.A. Bankaitis

PCR product was ligated into pGEM–T Easy Vector, yielding pGEM*spo20*. pGEM*spo20* was digested with *Sal*I and *Not*I and then ligated into same site of pREP1, yielding pREP1*spo20*.

Plasmids pREP1*SEC14* and pREP1*sec14*^{K66,239A} were constructed as follows. Two oligonucleotides were used to amplify either *SEC14* or *sec14*^{K66,239A} by PCR using 5′-CCCGTCGAC(*Sal*I)CATGGTTAC-ACAACAAGAAAAGGAATTTTT AGAATCC-3′ and 5′-CCCGAA-TTC(*Eco*RI)TCATTTCATCGAAAAGGCTTC-3′ as primers. The corresponding PCR products were subcloned into the pGEM–T Easy Vector, yielding pGEM*SEC14R*. pGEM*SEC14R* was then digested with *Sal*I and *Not*I and then subcloned into the corresponding sites of pREP1.

Plasmid pYES*spo20* was constructed by amplifying the *spo20* gene using 5′-CCCAAGCTT(*Hin*dIII)ATGTCAGAAACTATATCGG-3′ and 5′-CCCCTCGAG(*Xho*I)CTAATTTTTGTTCATCCAC-3′ as primers. The PCR product was digested with *Hin*dIII and *Xho*I and then subcloned into the corresponding sites of pYES2, yielding pYES*spo20*.

Finally, plasmids pYES*SEC14* and pYES *sec14*^{K66,239A} were constructed by amplifying *SEC14* and *sec14*^{K66,239A} using 5′-CCCAAGCTT(*Hin*dIII)ATGGTTACACAAGAAAAG-3′ and 5′-CCC-GAATTC(*Eco*RI)TCATTTCATCGAAAAGGCTTC-3′ as primers. The PCR product was then subcloned into the pGEM–T Easy Vector, yielding pGEM*SEC14Y*. pGEM*SEC14Y* was digested with *Hin*dIII and *Not*I and then subcloned into the corresponding sites of pYES2.

Gene Disruption of spo20

spo20^{+} was disrupted by inserting *ura4*$^{+}$ into the *spo20* coding region. A 3.6-kb *Xho*I–*Not*I fragment was subcloned into Bluescript-II KS^{+} (Stratagene, La Jolla, CA). The 1.8-kb *ura4*$^{+}$ fragment (Grimm *et al.*, 1988) was then inserted into the internal *Bam*HI site, yielding pYN4-U (see Figure 3A). A 5.3-kb *Hin*dIII–*Cla*I fragment containing the interrupted *spo20* allele (*spo20::ura4*$^{+}$) was used to transform the strain, YN15. Disruption was confirmed by Southern hybridization of genomic DNA.

Southern and Northern Analysis

Genomic DNA was restricted, fractionated in a 1.0% agarose gel, and then transferred onto nylon membranes (Biodyne A; Nihon Pall Co., Tokyo, Japan). Total RNA was prepared from *S. pombe* cultures (Jensen *et al.*, 1983) and fractionated on a 1.0% gel containing 3.7% formaldehyde as reported previously (Thomas, 1980).

Nucleotide Sequence Analysis of the spo20-KC104 allele

The entire *spo20* ORF was amplified by PCR using genomic DNA from the *spo20-KC104* mutant as a template and then cloned into Bluescript-II KS^{+}. The PCR primers used were 5′-CCCAAGCT-G(*Hin*dIII)ATGTCAGAAACTATATCGG-3′ and 5′-CCCCTCGAG-(*Xho*I)CTAATTTTTGTTCATCCAC-3′. The nucleotide sequences of three clones derived from independent PCR amplifications were determined in their entirety. Comparison of the nucleotide sequences of *spo20-KC104* with *spo20*$^{+}$ revealed a single nucleotide change, from G to A, which resulted in the replacement of glycine 275 with aspartate occurring in the *spo20-KC104* allele.

Western Blotting

The pIU(Δ5′-*spo20*)-HA plasmid carrying 5′-truncated *spo20* was linearized by restricting it with *Spe*I near the center of the *spo20* sequences and introduced into the YN8 strain (*h*^{90} *spo20-KC104* ura4-D18). Because *Ura*$^{+}$ transformants were obtained that were competent both for growth at 37°C and sporulation, we concluded that Spo20-HA is a functional protein. That this integrant strain (YN8-WH) harbors a single copy of *spo20*-HA at the *spo20* locus was confirmed by Southern hybridization. Likewise, pIU(Δ5′-

spo20^{G275D})-HA plasmid was integrated into the TN9 strain (*h*^{90} *ura4-D18*). The *Ura*$^{+}$ transformants were temperature sensitive and sporulation defective. Southern hybridization also confirmed that the transformant strain, YN8-MH, harbors a single copy of *spo20*^{G275D}-HA at the *spo20* locus. A wild-type strain (YN8-WH) and a *spo20* mutant strain (YN8-MH) were cultured in liquid sporulation medium (MM-N). At intervals, culture aliquots were collected, and crude cell extracts were prepared as described by Masai *et al*. (1995). Polypeptides were resolved by SDS-PAGE on 12.5% gels and then transferred onto polyvinylidene difluoride membranes (Millipore, Bedford, MA). Filters were probed with mouse anti-HA antibody 12CA5 (Boehringer Mannheim, Mannheim, Germany) at a 1:1000 dilution. Blots were also probed with anti-α-tubulin antibody, TAT-1 (Woods *et al.*, 1989), to normalize protein load. Immunoreactive bands were visualized by staining with horse radish-conjugated goat anti-mouse IgG (Promega, Madison, WI) and chemiluminescence (NEN Life Sciences, Boston, MA).

Determination of spo20 Phospholipid Transfer Activities

S. cerevisiae strain CTY303 is devoid of measurable endogenous PtdIns- and PtdCho-transfer activity. This strain was transformed with the appropriate YEp(*spo20*$^{+}$) and YEp(*SEC14*) plasmids and the control vector YEplac195. One liter cultures of these derivative strains were grown to midlogarithmic phase in uracil-free medium at 26°C, harvested by centrifugation, and finally resuspended in spheroplast buffer (1.1 M sorbitol, 10 mM Tris-HCl, pH 7.5). β-Mercaptoethanol was then added to a final concentration of 25 mM, after which cells were incubated at room temperature for 10 min, pelleted, and resuspended once more in spheroplast buffer. Oxalyticase (Enzogenetics; Corvallis, OR) was added (2 μg/ml), and enzymatic digestion of the yeast cell wall was allowed to proceed in a 1 h incubation at 30°C. Spheroplasts were then harvested by centrifugation at 500 × *g*, resuspended in 0.55 M sorbitol, 5 mM Tris-HCl, pH 7.5, 500 mM KCl, and 1 mM PMSF, and equal volumes of glass beads (0.5 mm) (Sigma, St. Louis, MO) were added to the spheroplast suspensions. Each suspension was subjected to eight 1-min bursts of vigorous vortexing with a 1-min rest on ice between each burst. Broken-cell extracts were clarified by a serial regimen of differential centrifugation at 1,000 × *g*, 13,000 × *g*, and 100,000 × *g*, respectively. The 100,000 × *g* supernatants were collected and subjected to a final clarification step of filtration through 0.45 μm Millipore (Millipore, Bedford, MA) filters. The filtrates were designated as cytosolic fractions, and protein concentrations were assayed using the BCA kit (Pierce, Rockford, IL). Bovine serum albumin was used as protein standard. PtdIns- and PtdCho-transfer assays were performed as described (Aitken *et al.*, 1990; Skinner *et al.*, 1993; Li *et al.*, 2000). [1,2-^{3}H(*N*)]-inositol, [^{14}C]-PtdCho, and [^{14}C]-SM were from American Radiolabeled Chemicals (St. Louis, MO). Other phospholipids were obtained from Avanti Polar Lipids (Alabaster, AL).

Immunofluorescence Microscopy

For cell fixation, we followed the procedure of Hagan and Hyams (1988) using glutaraldehyde and paraformaldehyde. The SPB was visualized by indirect immunofluorescence microscopy using rabbit anti-Sad1 antibody (a gift from O. Niwa, Kazusa DNA Research Institute) and Alexa 546-conjugated goat anti-rabbit IgG (Molecular Probes, Eugene, OR). The Spo20p-HA was visualized by indirect immunofluorescence microscopy using rat anti-HA antibody 3F10 (Boehringer Mannheim) and Alexa 488-conjugated goat anti-rat IgG (Molecular Probes). For costaining of F-actin, rhodamine-phalloidin (Molecular Probes) was added when the secondary antibody was applied. The nuclear chromatin region was stained with 4′, 6-diamidino-2-phenylindole (DAPI) at 1 μg/ml. Stained cells were observed under a fluorescence microscope (model BX50; Olympus, Tokyo, Japan).

Treatment with Latrunculin A

Wild-type strain YN8-WH carrying *spo20-HA* was grown to midlog phase in SSL at 28°C. Latrunculin A (Biomol Research Laboratories, Plymouth Meeting, PA) dissolved in DMSO at 10 mM was added to 3 ml cultures to a final concentration of 10 μM. Cells were incubated with the drug for 2 h and then fixed. Localization of Spo20-HA and F-actin was visualized as described above.

Electron Microscopy

Cells were mounted on the copper grids to form a thin layer and plunged into liquid propane cooled with liquid N_2. Frozen cells were transferred to 2% OsO_4 in anhydrous acetone, kept at −80°C for 48 h in a solid CO_2-acetone bath, then transferred to −35°C for 2 h, 4°C for 2 h, and room temperature for 2 h. After washing with anhydrous acetone three times, samples were infiltrated with increasing concentrations of Spurr's resin in anhydrous acetone and finally with 100% Spurr's resin. These samples were then polymerized in capsules at 50°C for 5 h and 60°C for 50 h. Thin sections were cut on a Reichest Ultracut S and then stained with uranyl acetate and lead citrate. Sections were viewed on a JEOL 2010 electron microscope at 100 kV.

RESULTS

spo20-KC104 Mutant Completes Meiosis, but Does Not Form Spores

As we reported previously, *spo20-KC104* mutants are defective in ascospore formation (Kishida and Shimoda, 1986; Hirata and Shimoda, 1992). To investigate meiosis and sporulation in *spo20-KC104* mutants in more detail, we monitored meiotic nuclear divisions and ascus formation in these mutants. Homozygous diploid strains YN47–53 (wild type) and YN13–14 (*spo20-KC104*) were used to increase synchrony. Cells grown in the presence of a nitrogen source (SSL+N) were transferred and incubated in sporulation medium (SSL-N medium) at 25°C. Culture aliquots were collected every hour after shift, and cells were stained with DAPI. Mono-, bi-, and tetra-nucleate cells were then counted (Figure 1A). First and second meiotic divisions in the *spo20-KC104* mutant proceeded with kinetics similar to those recorded for the isogenic wild-type strain (Figure 1A); however, although the final yield of asci reached ~90% in the wild-type strain, virtually no asci were observed in the *spo20-KC104* strain (Figure 1B). These results suggest that *spo20-KC104* mutant is able to complete meiosis but is defective in ascospore formation.

spo20-KC104 Shows Temperature-Sensitive Growth and Is Defective in Cell Separation at the Restrictive Temperature

In addition to ascospore formation, we found that the *spo20-KC104* mutation compromised vegetative growth. As shown in Figure 2A, the *spo20-KC104* mutant grew well at 25°C but was unable to form colonies at 37°C. Thus, *spo20-KC104* confers temperature sensitivity for growth. We therefore examined the cell morphology of *spo20-KC104* mutants incubated at permissive and restrictive temperatures. Because actin distribution and septum formation are important for the determination of cell shape and for growth polarity of fission yeast (Marks and Hyams, 1985; Marks *et al.*, 1986), these parameters were monitored by staining with rhodamine-phalloidin and calcofluor, respectively. We noted that

spo20 mutants were indistinguishable from wild-type cells in both actin distribution and septum formation when incubated at 25°C (Figure 2B). In marked contrast, *spo20* cells exhibited a rather uniform arrest morphology at the restrictive temperature. At 12 h after shift to 37°C, some 60% of the *spo20* cells had a single septum, whereas 8% exhibited multiple septa. Only 13% of the wild-type cells were septated (Table 2). Moreover, cortical actin localized either to growing tips or to the division plane of wild-type cells, as reported previously (Marks and Hyams, 1985; Marks *et al.*, 1986); however, in most of the *spo20* cells, cortical actin patches failed to localize to cell tips and were dispersed randomly (Figure 2B). These results suggest that *spo20*$^+$ is required for normal cell division of vegetative cells, most likely for completion of septation.

The spo20$^+$ *Gene Encodes a Fission Yeast Homologue of Budding Yeast Sec14*

The *spo20*$^+$ gene was cloned by functional complementation of *spo20-KC104*. From a screen of ~15,000 colonies transformed with an *S. pombe* genomic library constructed in the pFL20 (Losson and Lacroute, 1983), we recovered two plasmids that complemented both the temperature sensitivity and the sporulation deficiency of the *spo20* mutant. Subcloning indicated that the complementing activities of these plasmids were associated with a 2.1-kb *Fba*I fragment (Figure 3A). Partial DNA sequencing of this insert revealed that it was derived from a region of chromosome I that had been sequenced by the *S. pombe* genome project (cosmid SPAC3H8; EMBL/GenBank/DDBJ accession No. Z69086). The cloned fragment contained only one ORF, SPAC3H8.10. The same gene was isolated in independent complementation screens using two independent cDNA libraries.

To confirm that the cloned gene was indeed *spo20*$^+$, the isolated gene was recloned into an integration vector (pTN22) carrying *ura4*$^+$ as a selective marker. This plasmid was then integrated into the fission yeast genome by homologous recombination. Tetrad analysis of the heterozygous diploid constructed by crossing the haploid integrant strain with a *spo20-KC104* mutant showed that the Ura$^+$ and Spo$^+$ phenotypes cosegregated. This result indicates that the cloned gene is *spo20*$^+$ itself and not a dosage suppressor.

From the nucleotide sequence, we infer that *spo20*$^+$ encodes a protein of 286 residues and a molecular mass of 32.7 kDa. BLAST searches against various databases (EMBL/GenBank/DDBJ) showed that Spo20 shares 54.5% identity and 76.6% similarity with budding yeast Sec14p (Figure 3, C and D), and the Spo20 primary sequence is identical to that of the *S. pombe* Sec14p homologue that had been reported previously (Bankaitis *et al.*, 1989; Skinner *et al.*, 1995; Kearns *et al.*, 1998a). Budding yeast Sec14p has intrinsic PtdIns- and PtdCho-transfer activity in vitro, associates with Golgi membranes in vivo, and is required for transport of secretory proteins from the yeast Golgi apparatus (Bankaitis *et al.*, 1989, 1990; Cleves *et al.*, 1991; Kearns *et al.*, 1998b).

Spo20 Is Essential for Cell Viability

To determine the consequences of complete loss of *spo20*$^+$ function, we constructed a plasmid in which the *ura4*$^+$ cassette was inserted at the *Bam*HI site within the *spo20*$^+$ ORF (Figure 3A). After transformation of the *S. pombe* diploid

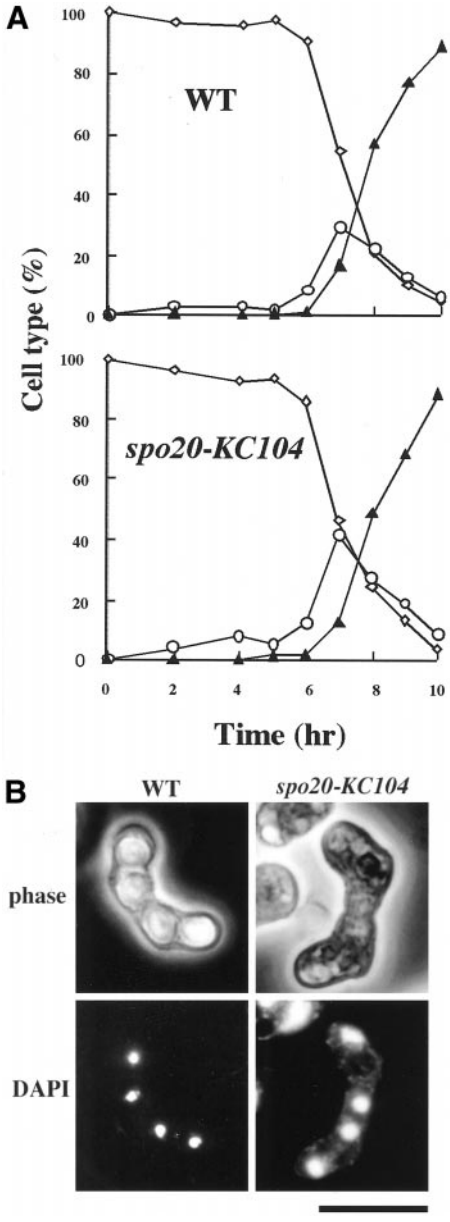

Figure 1. The *spo20-KC104* mutant is defective in sporulation. (A) Kinetics of meiosis in a wild-type (WT) and a *spo20-KC104* mutant. YN13–14 (*h*$^+$/*h*$^-$ *spo20-KC104/spo20-KC104 ade6-M210/ade6-M216*) and YN49–53 (*h*$^+$/*h*$^-$ *ade6-M210/ade6-M216*) precultured overnight in liquid growth medium (SSL+N) were incubated with shaking at 25°C in liquid sporulation medium (SSL-N). A portion of the culture was stained with DAPI. Meiotic cells were classified by the number of nuclei per cell. For each sample, ~500 cells were counted. This figure is depicted on the basis of one representative result of four independent experiments that provided similar results. Diamonds, mononucleate cells; circles, binucleate zygotes; triangles, trinucleate or tetranucleate cells. (B) DAPI image of *spo20-KC104* during sporulation. YN10 (*spo20-KC104*) and YN12 (WT) were incubated at 25°C in sporulation medium (MEA) for 24 h. Chromosomal DNA was stained with DAPI. Bar, 10 μm.

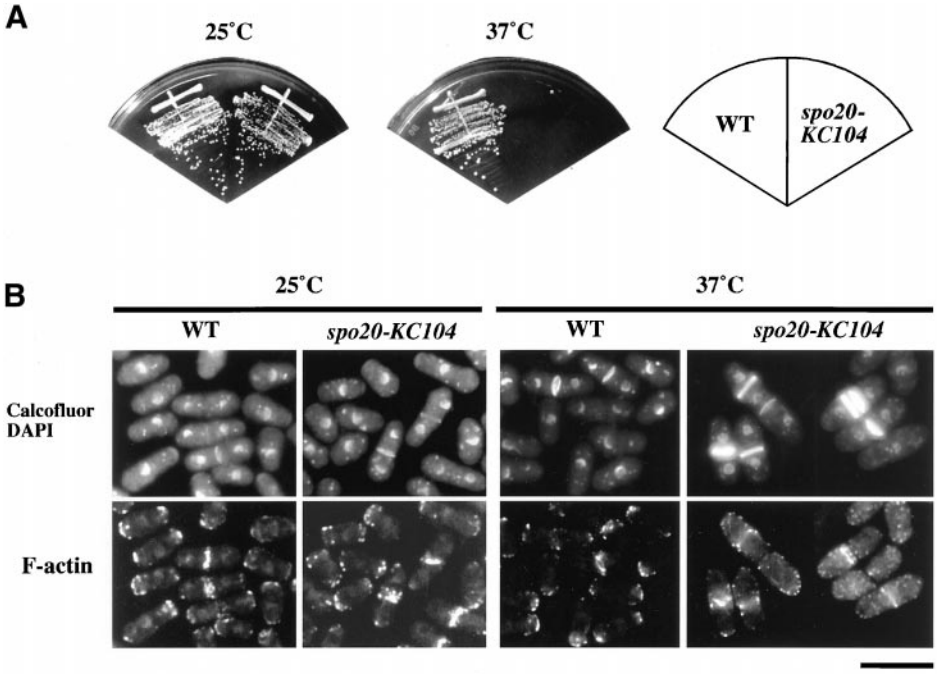

Figure 2. The *spo20-KC104* mutant exhibits temperature-sensitive growth. (A) Strains YN10 (*spo20-KC104*) and YN12 (WT) were streaked on complete medium (YEA) and incubated at 25 or 37°C for 5 d. (B) Cell morphology at nonpermissive temperatures. YN10 and YN12 were incubated in liquid complete medium (YEL) for 12 h at 25 or 37°C. Cells were fixed and stained with Alexa 568-conjugated phalloidin, calcofluor, and DAPI. Bar, 10 μm.

strain YN15 with a linear DNA fragment containing the disrupted allele of *spo20*$^+$, Ura$^+$ transformants were obtained. Tetrad analysis indicated that every ascus consisted of two viable and two inviable spores, and that all viable spores were phenotypically Ura$^-$ (Figure 3B). Microscopic observation of nonviable meiotic progeny showed that these spores germinated but ceased growth soon thereafter. Therefore, *spo20*$^+$ is essential for vegetative cell growth and viability.

Sequence Analysis of spo20-KC104

To determine the precise identity of the *spo20-KC104* allele, the mutant gene was isolated from genomic DNA by PCR amplification (see MATERIALS AND METHODS). Nucleotide sequence analyses demonstrated that *spo20-KC104* is the result of a single nucleotide change (from G to A) that caused replacement of glycine 275 with asparatate in the conserved C-terminal region (Figure 3D). We refer to the protein product of *spo20-KC104* as Spo20^{G275D}. This missense substitution likely disrupts a 3_{10}-helix that resides within a string motif that itself stabilizes the large hydrophobic phospholipid binding pocket of Sec14p-like proteins (Sha *et al.*, 1998). The classical *sec14–1*^{ts} allele results in a $G_{266}D$ missense substitution (Cleves *et al.*, 1989), and this substitution disrupts a distinct 3_{10}-helix that also resides within that same string motif (Sha *et al.*, 1998).

Table 2. Cell morphology of wild-type and *spo20-KC104* strains

	Frequency (%)			
	WT		*spo20-KC104*	
Cell type	25°C	37°C	25°C	37°C
Nonseptated cells	87.3	86.7	90.1	32.1
Normally septated cells	12.3	13.1	8.9	59.8
Abnormal septated cells	0.4	0.3	1.0	8.1

YN10 and YN12 were incubated in liquid complete medium (YEL) for 12 h at 25 or 37°C. Cells were fixed and stained with calcofluor and DAPI. For each sample, ~500 cells were counted. This experiment was performed three times, and the results were reproducible. The results presented are from a representative single experiment.

spo20$^+$ *Expression Is Constitutive*

We also studied the expression of *spo20*$^+$. Generally, the *S. pombe* genes responsible for mating, meiosis, and sporulation are transcribed under conditions of nutritional starvation (reviewed by Yamamoto *et al.*, 1997); however, Northern analyses revealed that *spo20*$^+$ transcription occurred during vegetative growth and was not enhanced further after the shift to a nitrogen-free medium (Figure 3E). This result is consistent with the view that Spo20 is essential for vegetative growth.

Spo20 Is a Functional Homologue of the Budding Yeast Sec14

To assess the level of functional relatedness between Spo20 and budding yeast Sec14p, *spo20*$^+$ was expressed under control of the *GAL1* promoter in *sec14-1*^{ts} mutants of *S. cerevisiae*. Ectopic expression of *spo20*$^+$ clearly rescued the temperature sensitivity for growth phenotype of *sec14-1*^{ts} mutants (Figure 4A). In other experiments, we also discovered that *spo20*$^+$ expression complements the unconditional lethality associated with *sec14* null mutations in budding

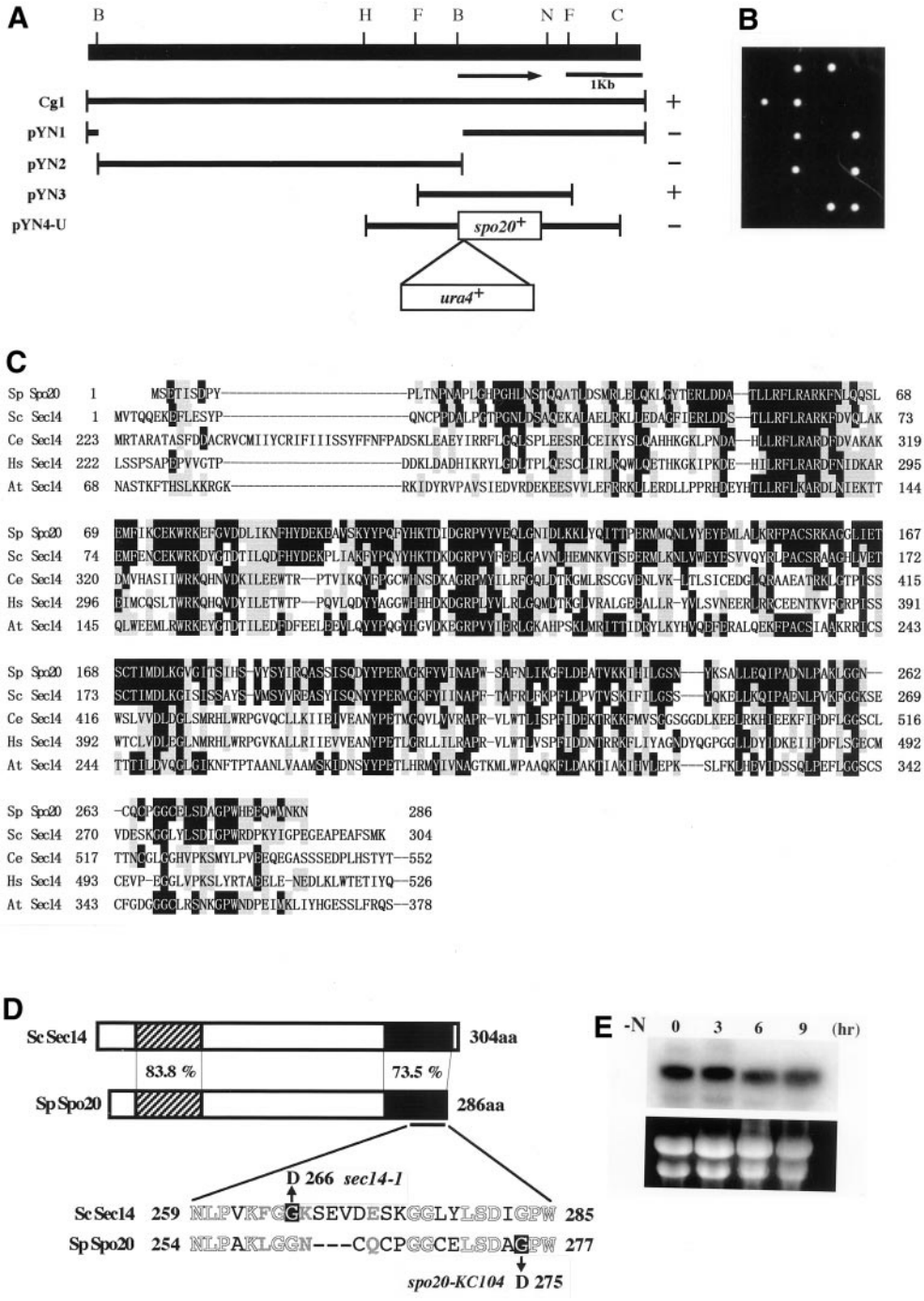

Figure 3. Structure of the *spo20*$^+$ gene. (A) Restriction map, subcloning, and construction of null mutants. The arrow indicates the region and direction of the *spo20*$^+$ ORF, which encodes a protein composed of 286 amino acid residues. All the subclones were derived from Cg1. Complementation by each subclone: +, complements; −, does not complement. Restriction enzyme sites: B, *Bam*HI; C, *Cla*I; F, *Fba*I; H, *Hin*dIII; N, *Nco*I. (B) Viability of *spo20::ura4*$^+$ spores. A diploid (YN16) heterozygous at the *spo20* locus (+/*spo20::ura4*$^+$) was sporulated, and the dissected tetrads were incubated on YEA plates at 25°C for 5 d. (C) Comparison of the amino acid sequences of Spo20 and other members of the Sec14 family. Identical amino acids are shown in white against black, and similar amino acids are shaded. Sp, *S. pombe* (286 aa); Sc, *S. cerevisiae* (304 aa); Ce, *Caenorhabditis elegans* (743 aa); Hs, *Homo sapiens* (715 aa); At, *Arabidopsis thaliana* (648 aa). (D) Schematic representation of the structures of Spo20 and Sec14. The overall identity and similarity between Spo20 and Sec14 are 54.5 and 76.6%, respectively. The amino acid similarities between them in the N-terminal (hatched) and C-terminal (filled) conserved domains are also shown. The *spo20-KC104* mutant allele carries a single nucleotide change (from G to A) that results in the replacement of glycine 275, as shown by white against black, with asparatate. For comparison, the mutation site of *sec14-1*^{ts} is also shown (Cleves *et al.*, 1989). Identical amino acids are represented by white letters, and similar amino acids are represented by gray ones. (E) Northern analysis. L968 precultured in growth medium (MM+N) was incubated in liquid sporulation medium (MM-N) at 25°C. After the shift, samples were taken and subjected to Northern blotting. Top, *spo20*$^+$ mRNA; bottom, rRNA stained with ethidium bromide.

yeast. These data establish that fission yeast Spo20 is able to fulfill all essential Sec14 functions when expressed in budding yeast.

To execute the reciprocal experiment, *S. cerevisiae SEC14* was placed under control of the thiamine-repressible *nmt* promoter and introduced into an *S. pombe spo20* mutant. This expression plasmid, pREP1*SEC14*, rescues both the temperature sensitivity for growth and the Spo$^-$ phenotypes of the *spo20* mutant even in the presence of thiamine, which represses the transcription (Figure 4, B and C). The level of suppression of sporulation deficiency realized by *SEC14* expression was comparable to that achieved by expression of *spo20*$^+$ (Figure 4D), and the spores produced in *SEC14*-expressing strains were viable (Figure 4E). Finally, pREP1*SEC14* rescued all morphological defects associated with the *spo20* mutant. These results indicate that *S. pombe* Spo20 is not only a structural homologue but is also a functional homologue of *S. cerevisiae* Sec14.

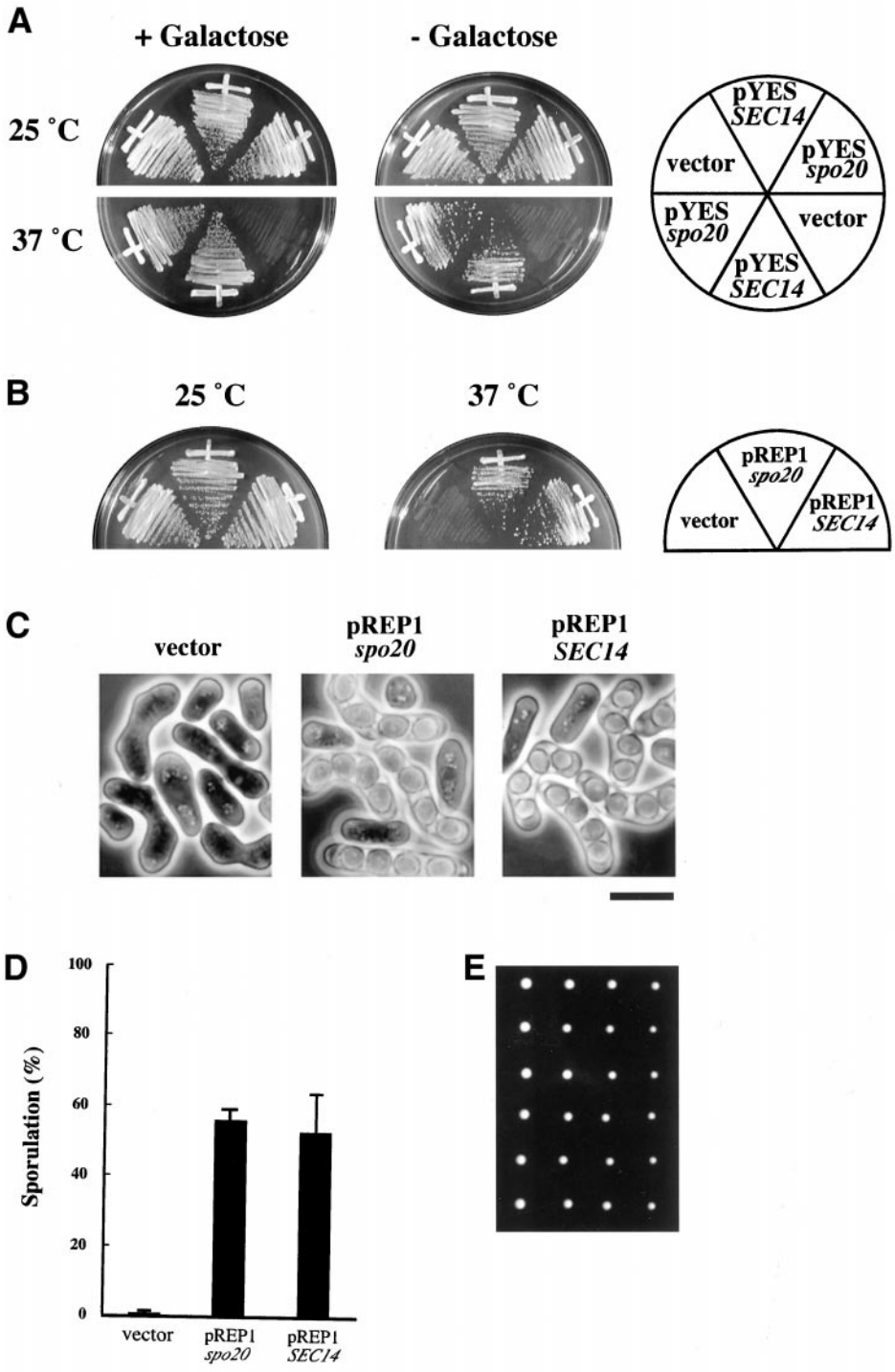

Figure 4. Spo20 is a functional homologue of Sec14. (A) Overexpression of *S. pombe spo20*$^+$ suppressed *S. cerevisiae sec14–1*^{ts}. A multicopy plasmid carrying *spo20*$^+$ (pYES*spo20*) was transformed into an *S. cerevisiae sec14–1*^{ts} mutant. The Ura$^+$ transformants were incubated in YP-Glucose and YP-Galactose for 3 d at 25 or 37°C. (B) Overexpression of *S. cerevisiae SEC14* suppressed the temperature sensitivity of *spo20-KC104*. Strain YN11 (*spo20-KC104*) was transformed with an empty pREP1, pREP1*SEC14*, or pREP1*spo20*. The Leu$^+$ transformants were incubated in complete medium (YEA) at 25 or 37°C for 5 d. (C) Suppression of sporulation defect in *spo20-KC104* by *S. cerevisiae SEC14*. The Leu$^+$ transformants with pREP1, pREP1*SEC14*, or pREP1*spo20* were incubated in sporulation medium (MEA) at 25°C for 2 d. Bar, 10 μm. (D) Sporulation efficiency of the transformants. The Leu$^+$ transformants with an empty pREP1, pREP1*SEC14*, or pREP1*spo20* were incubated in MEA at 25°C for 2 d. (E) Viability of spores produced by *SEC14*-driven sporulation. A homozygous diploid carrying pREP1*SEC14* was sporulated, and the dissected tetrads were incubated on complete medium (YEA) at 25°C for 5 d.

Spo20 Protein Exhibits Both PtdIns- and PtdCho-transfer Activity

In budding yeast, phospholipase D (PLD) is required for completion of the sporulation program. PLD-deficient mutants resemble *S. pombe spo20* mutants in that these are defective in forespore membrane formation (Rose *et al.*, 1995; Rudge *et al.*, 1998). Four novel budding yeast PITPs, which share limited primary sequence homology with Sec14, are collectively required for optimal PLD activation in vegetative cells (Li *et al.*, 2000). These novel PITPs, designated Sfh proteins, are nonclassical PITPs. That is, Sfh proteins exhibit

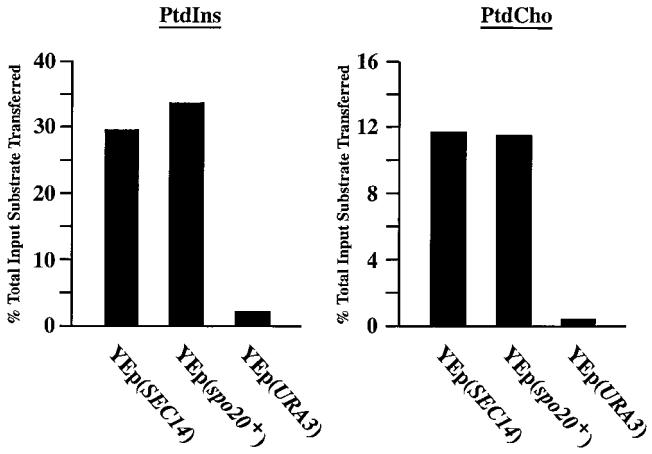

Figure 5. The *spo20*$^{+}$ gene product is a PtdIns/PtdCho-transfer protein. Relative abilities of budding yeast Sec14 and Spo20 to transfer [^{3}H]PtdIns and [^{14}C]PtdCho were measured in crude cytosolic fractions prepared from *S. cerevisiae*. Activities are represented as the percentage of total input radiolabeled substrate transferred from donor membranes to unlabeled acceptor membranes. Transfer substrate for each data set is identified at top. In all cases, cytosol was clamped at 0.25 mg per assay. Sec14 and Spo20 were individually expressed in the *S. cerevisiae* strain CTY303 (see MATERIALS and METHODS), which has no detectable endogenous PtdIns- or PtdCho-transfer activity. Cytosol prepared from the isogenic YEp(*URA3*) derivative of strain CTY303 (i.e., strain CTY808) served as negative control. Sources of cytosol are identified at the bottom by the expression plasmids introduced into strain CTY303. Corresponding transfer values from mock assays were subtracted from each reaction. Mock samples represented the addition of buffer alone to each transfer reaction. In these experiments, input [^{3}H]PtdIns and [^{14}C]PtdCho ranged from 14639–19101 to 22428–27656 cpm for each assay, respectively. Background values in mock reactions ranged from 544–657 cpm for PtdIns-transfer assays to 1389–1489 cpm for PtdCho-transfer assays. These data are from a representative experiment.

PtdIns-transfer activity, but not PtdCho-transfer activity, in vitro (Li *et al.*, 2000). Interestingly, Sec14 itself is not required for PLD activation in budding yeast. It was therefore of direct interest to determine whether Spo20 is a classical or a nonclassical PITP.

Spo20 was expressed in the *cki1*, *sec14*Δ budding yeast strain CTY303, and we assayed cytosol prepared from this strain for PtdIns- and PtdCho-transfer activity. The Sec14-deficient CTY303 is an ideal host for this experiment because it lacks detectable endogenous PtdIns- and PtdCho-transfer activity. As a result, this strain does not contribute to signal even when crude cytosol preparations are analyzed (Cleves *et al.*, 1991; Skinner *et al.*, 1993; Kearns *et al.*, 1998a; Li *et al.*, 2000). The strain is viable because *cki1* effects a bypass of the normally essential Sec14 requirement for secretory pathway function and cell growth in budding yeast (Cleves *et al.*, 1991).

The YEp(*spo20*$^{+}$) plasmid used as Spo20 expression vehicle in these experiments was recovered from the pDB20-based *S. pombe* cDNA library of Beckers *et al.* (1991) where the cDNAs are placed under the transcriptional control of the powerful and constitutive promoter of the budding yeast alcohol dehydrogenase structural gene (P_{ADH1}) of budding yeast. In this manner, a number of YEp(*spo20*$^{+}$) plasmids were recovered by selecting for clones that complement the growth and secretory defects associated with the budding yeast *sec14-1*^{ts} mutation at 37°C. Nucleotide sequence analysis confirmed that the chosen representative, designated pCTY61, harbors a full-length *spo20*$^{+}$ cDNA positioned downstream of P_{ADH1}.

The PtdIns- and PtdCho-transfer data are shown in Figure 5. The YEp(*SEC14*) derivative strain served as positive control for PtdIns- and PtdCho-transfer, and cytosol prepared from this strain exhibited high levels of transfer for both of these phospholipid substrates. Incorporation of a rather low quantity of YEp(*SEC14*) cytosol into the assay (0.25 mg) resulted in the in vitro transfer of ~29.0 and 11.8% of the total input of [^{3}H]PtdIns and [^{14}C]-PtdCho from donor to acceptor membranes, respectively. By contrast, we failed to record significant PtdIns- or PtdCho-transfer activity in cytosol prepared from the CTY303/YEplac195 negative control strain (CTY808). Cytosol prepared from the YEp(*spo20*$^{+}$) strain, however, exhibited levels of both PtdIns- and PtdCho-transfer activity that were comparable to those measured in Sec14-containing cytosol (Figure 5). YEp(*spo20*$^{+}$) cytosol (0.25 mg) catalyzed the transfer of 33.6 and 11.4% of total input of [^{3}H]PtdIns and [^{14}C]-PtdCho substrate from donor to acceptor membranes, respectively. These biochemical data, although not allowing direct comparisons of specific Sec14 and Spo20 activities for PtdIns- and PtdCho-transfer, nonetheless unambiguously demonstrate that Spo20 is a classical PITP in that it exhibits both PtdIns- and PtdCho-transfer activities.

Because Spo20 is a classical PITP, we considered the idea that the PtCho-transfer activity of Spo20 is a functionally important activity in vivo. To test this possibility, we assessed whether expression of *S. cerevisiae* Sec14p^{K66,239A} could rescue *spo20*-associated phenotypes. Sec14p^{K66,239A} was used in this heterologous complementation experiment because this mutant protein, although specifically defective in PtdIns-transfer activity, is nonetheless functional in vivo (Phillips *et al.*, 1999). Interestingly, we found that Sec14^{K66,239A} expression complemented the sporulation deficiency of *S. pombe spo20-KC104* cells but failed to complement the temperature-sensitive growth phenotype. This observation suggests that the PtdIns-transfer activity, although apparently dispensable for sporulation-related Spo20 functions in *S. pombe*, appears to be essential for at least one critical vegetative function.

spo20-KC104 Mutant Accumulates Golgi Cisternae

Budding yeast *sec14* mutants are interpreted to be defective in vesicle budding from the yeast Golgi complex on the basis that these mutants exhibit a marked accumulation of Golgi bodies in the cytoplasm at nonpermissive temperature (Novick *et al.* 1980; Hirata, unpublished observations). Because *spo20* mutants suffer septation and sporulation defects, it was of interest to determine whether Spo20 is also involved in protein transport from the fission yeast Golgi complex. To this end, wild-type and mutant cells were incubated at a temperature restrictive for *spo20-KC104* mutants (35°C) for 6 h, and the terminal phenotypes of the *spo20-KC104* mutant were examined by electron microscopy. As shown in Figure 6, we observed a clear accumulation of Golgi cisternae in the cytoplasm of *spo20* cells. These results suggest that, as is the case for budding yeast Sec14, the *spo20*

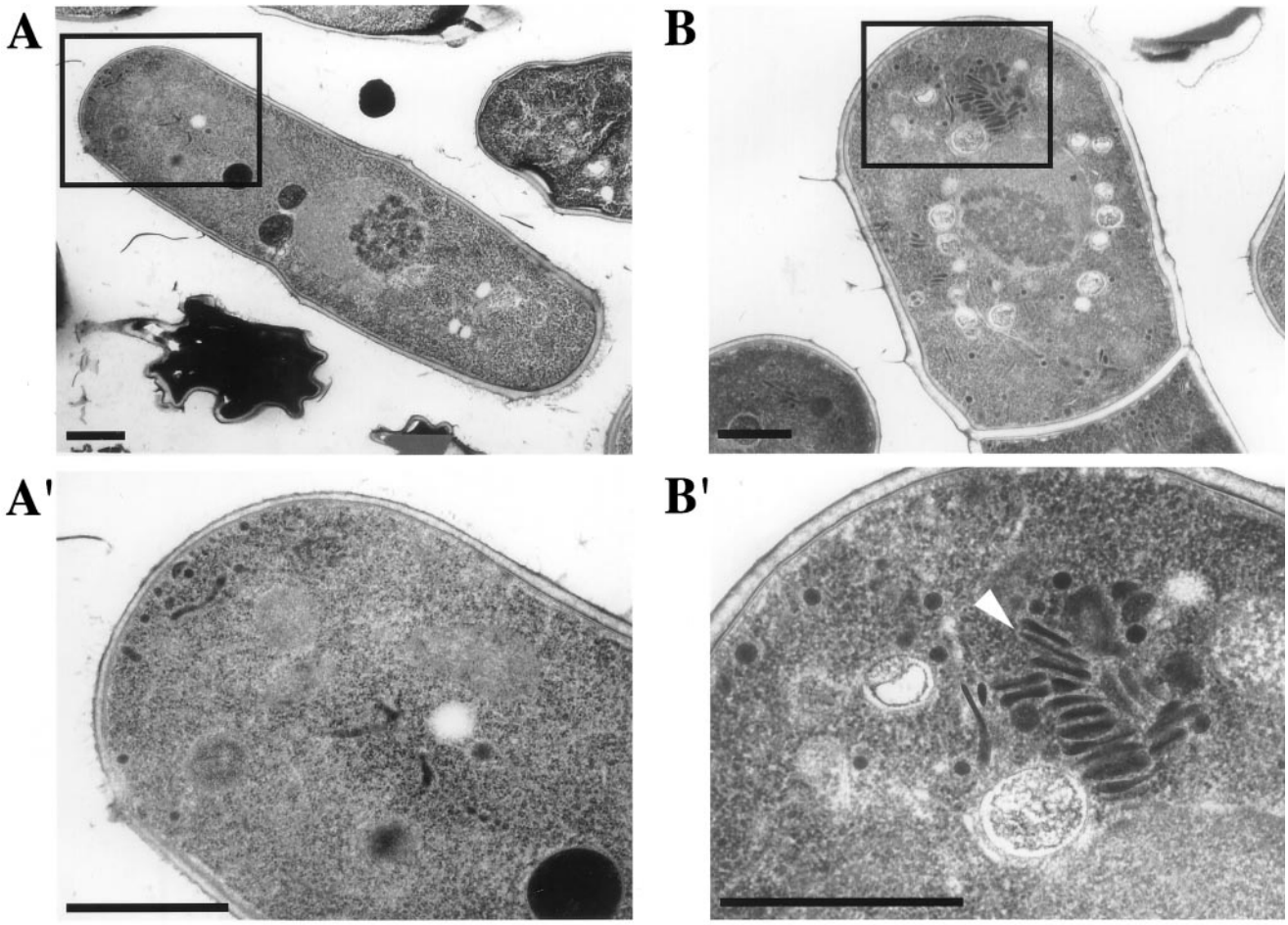

Figure 6. Accumulation of Golgi cisternae in *spo20-KC104* at restrictive temperature. YN10 (*spo20-KC104*) and YN12 (wild-type) cells cultured in liquid complete medium (YEL) for 6 h at 35°C were observed by electron microscopy. A and A′, a wild-type strain; B and B′, a *spo20-KC104* strain. A′ and B′ are magnified images of boxed parts of A and B, respectively. An arrowhead in B′ indicates accumulated Golgi cisternae. Bars, 1 μm.

mutant exhibits morphological phenotypes consistent with defects in protein trafficking from the fission yeast Golgi complex.

Immunological Detection of the Spo20 Protein

Because of the involvement of Spo20 in septation, Golgi function, and sporulation, we sought to determine the intracellular distribution of Spo20. To this end, we used strain YN8-WH, which carries a single chromosomal copy of the *spo20*$^{+}$ gene tagged with three tandem copies of an HA epitope (Figure 7A). YN8-WH grew at wild-type rates and sporulated at a wild-type efficiency as well. Thus, Spo20-HA scores as a fully functional protein.

Western analyses revealed that Spo20-HA resolves as a 39-kDa polypeptide on SDS-PAGE (Figure 7B). This apparent molecular mass corresponds well with that inferred from nucleotide sequence data. As shown in Figure 7B, we detected Spo20-HA in vegetative cells (0 h), and the abundance of this protein remained essentially constant after shift of cells to nitrogen-limited sporulation medium. To detect Spo20^{G275D}, we also constructed a strain expressing Spo20^{G275D}-HA (Figure 7A). The phenotypes of that strain are indistinguishable from those of the *spo20-KC104* mutant. Spo20^{G275D} was constitutively expressed, and steady-state levels of Spo20^{G275D}-HA were comparable to those of wild-type Spo20-HA. We did note that Spo20^{G275D}-HA SDS-PAGE mobility is slightly less than that seen for Spo20-HA (Figure 7B). Presumably this is because the mutant protein binds less SDS under denaturing conditions than does wild-type Spo20. Nevertheless, these results do suggest that phenotypes of the *spo20-KC104* mutant are not simply due to wholesale lability of Spo20^{G275D}.

Localization of the Spo20 Protein

We used immunofluorescence microscopy to assess the subcellular localization of Spo20-HA (Figures 8 and 9). In vegetative cells, Spo20-HA was predominantly localized in two distinct regions: cell tips in interphase cells and in the medial

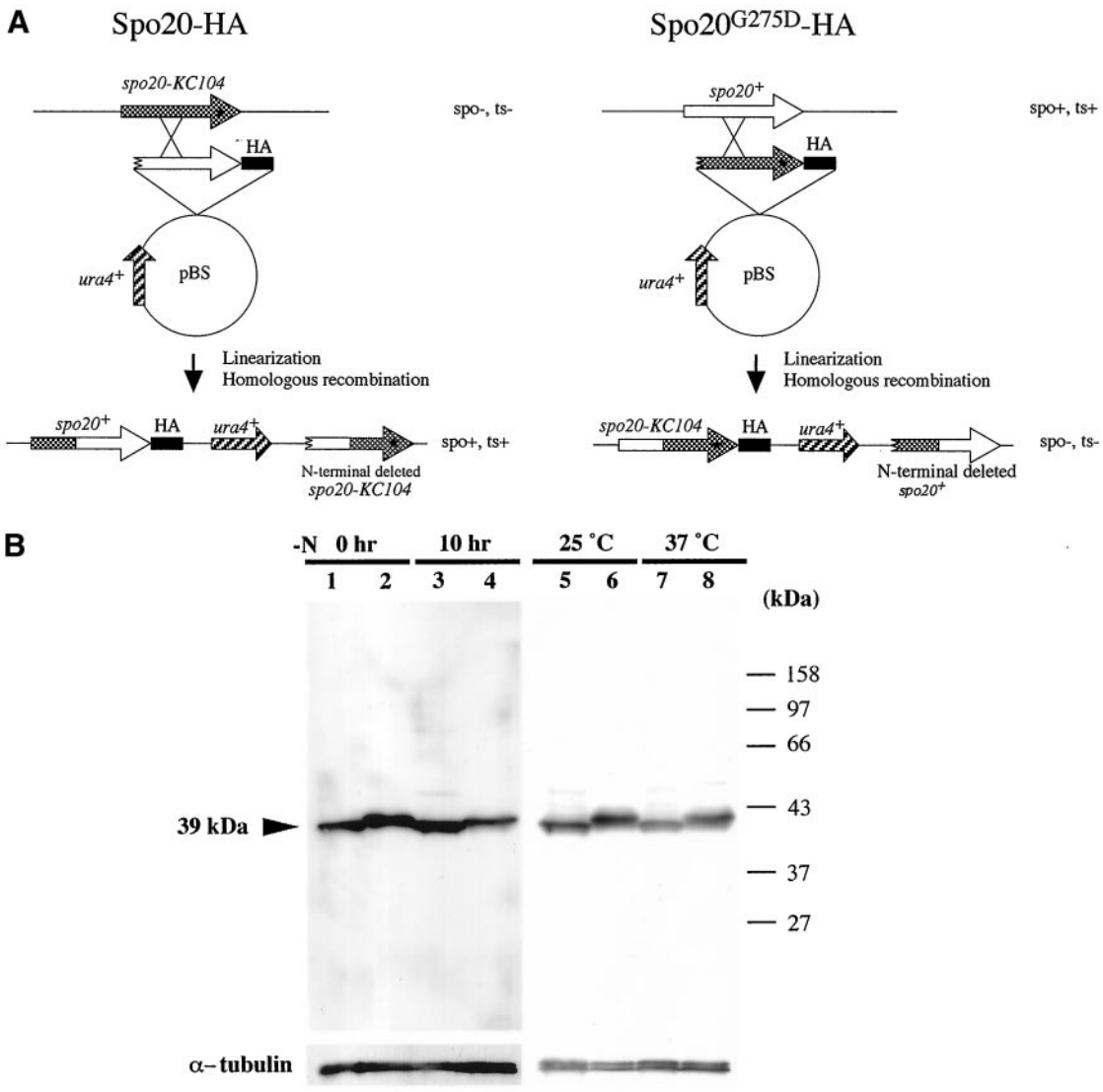

Figure 7. Detection of Spo20 and Spo20^{G275D} by Western blotting. (A) Strategy for constructing the *spo20-HA* and *spo20^{G275D}-HA* fusion genes. (B) Western blotting analysis of Spo20 and Spo20^{G275D}. Wild-type strain (YN8-WH) and *spo20* mutant strain (YN8-MH) carrying *spo20-HA* and *spo20^{G275D}-HA*, respectively, were cultured in liquid sporulation medium (MM-N) at 25°C. Protein extracts were prepared at 0 and 10 h (lanes 1–4). Cells were also cultured in liquid complete medium (YEL) at 25 or 37°C for 12 h (lanes 5–8). Protein extracts were subjected to immunoblot analysis with the mouse anti-HA, as well as with anti-α-tubulin antibody as the loading control. Lanes 1, 3, 5, and 7, Spo20-HA; lanes 2, 4, 6, and 8, Spo20^{G275D}-HA. Spo20-HA was detected as a band of ~39 kDa.

region in mitotic cells. During the G2 phase of the cell cycle, tip cell extension occurs first at the "old" end, and then the new end gains the capacity to grow. When cells enter M-phase, extension growth ceases and the septum is constructed (Mitchison and Nurse, 1985). To analyze Spo20-HA localization in greater detail, we monitored Spo20-HA localization at different stages of the cell cycle. Immediately after cell separation, Spo20-HA was more concentrated at the new cell end relative to the old cell end. During G2 phase, some Spo20-HA distributed to the old cell end so that both cell ends were stained rather evenly. In late mitosis when actin rings have already been constructed, Spo20-HA accumulated at a medial septum site, and Spo20-HA staining split into two plates before cell separation. Spo20-HA still remained at the tips of the dividing cell, although the intensity of staining decreased (Figure 8A). The collective data suggest that Spo20-HA is present at both cell poles throughout the cell cycle, whether cells are growing or not, and also in a medial region at mitosis (Figure 8A).

To address whether the actin cytoskeleton is required for localization of Spo20, F-actin was depolymerized by treatment of cells with latrunculin A, and Spo20-HA localization was then determined. As shown in Figure 8B, after a 2-h incubation with latrunculin A, Spo20-HA localization to both the cell pole and medial regions was abolished. Spo20-HA localization was not affected by depolymerization

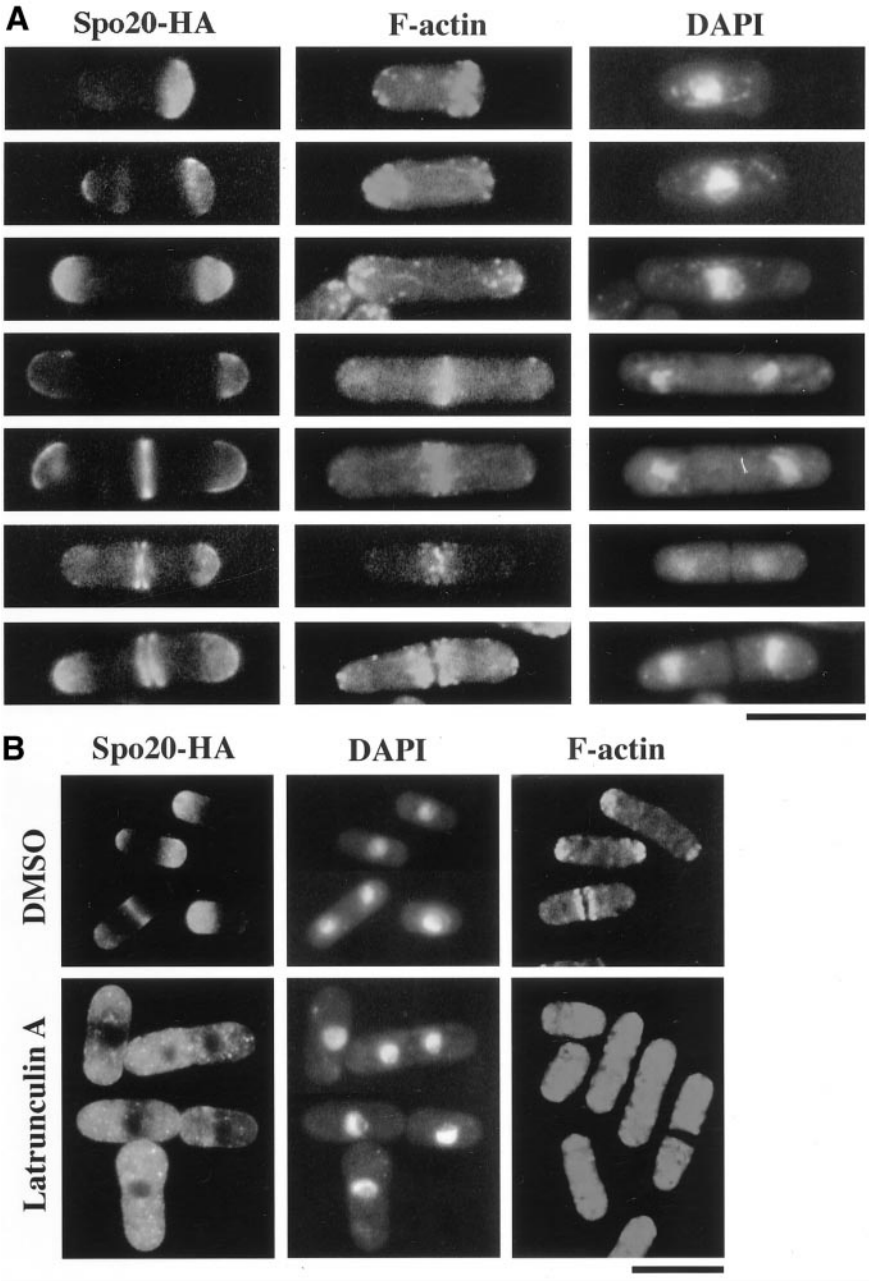

Figure 8. The Spo20 localizes in close proximity to the F-actin cytoskeleton in vegetative cells. (A) Fluorescence microscopy using anti-HA and rhodamine-phalloidin. Wild-type strain YN8-WH carrying *spo20-HA* was grown to midlog phase in SSL at 28°C and then fixed. Cells were stained with anti-HA antibody to detect Spo20, with rhodamine-phalloidin to detect F-actin and with DAPI to visualize nuclear chromatin regions. (B) Disruption of the Spo20 localization by depolymerization of the F-actin cytoskeleton. Wild-type strain YN8-WH carrying *spo20-HA* was treated with latrunculin A for 2 h. Cells were processed for immunofluorescence microscopy to visualize F-actin and Spo20 and to stain nuclear chromatin regions. Bars, 10 μm.

of microtubules by the treatment with TBZ. These results suggest that F-actin assembly is essential for proper localization of Spo20-HA.

We also investigated Spo20 localization during meiosis and sporulation. Interestingly, the localization of Spo20-HA changed markedly. After the shift to nitrogen-free medium, Spo20-HA immediately translocated into the nucleus (Figure 9A). The nuclear localization was maintained through conjugation and meiosis. The nuclear Spo20-HA pool, however, diminished as cells proceeded through meiosis II. After meiosis II was completed, Spo20-HA localized to the prespore periphery (Figure 9A). We recently found that the Spo3 protein required for sporulation localized to forespore membranes during meiosis (Kubo, Nakamura, and Shimoda, unpublished observations). To elucidate whether Spo3 and Spo20 colocalize to forespore membranes, sporulation was induced in cells expressing green fluorescent protein (GFP)-tagged Spo3 and Spo20-HA. As shown in Figure 10, Spo20-HA distribution was coincident with that of Spo3-GFP on the prespore surface. Spo20^{G275D}-HA localization resembles that of wild-type Spo20-HA throughout vegetative growth and meiosis (Figure 9B). Therefore, it is unlikely that phenotypes of the *spo20-KC104* mutant are simply due to mislocalization of Spo20 (Figure 9B).

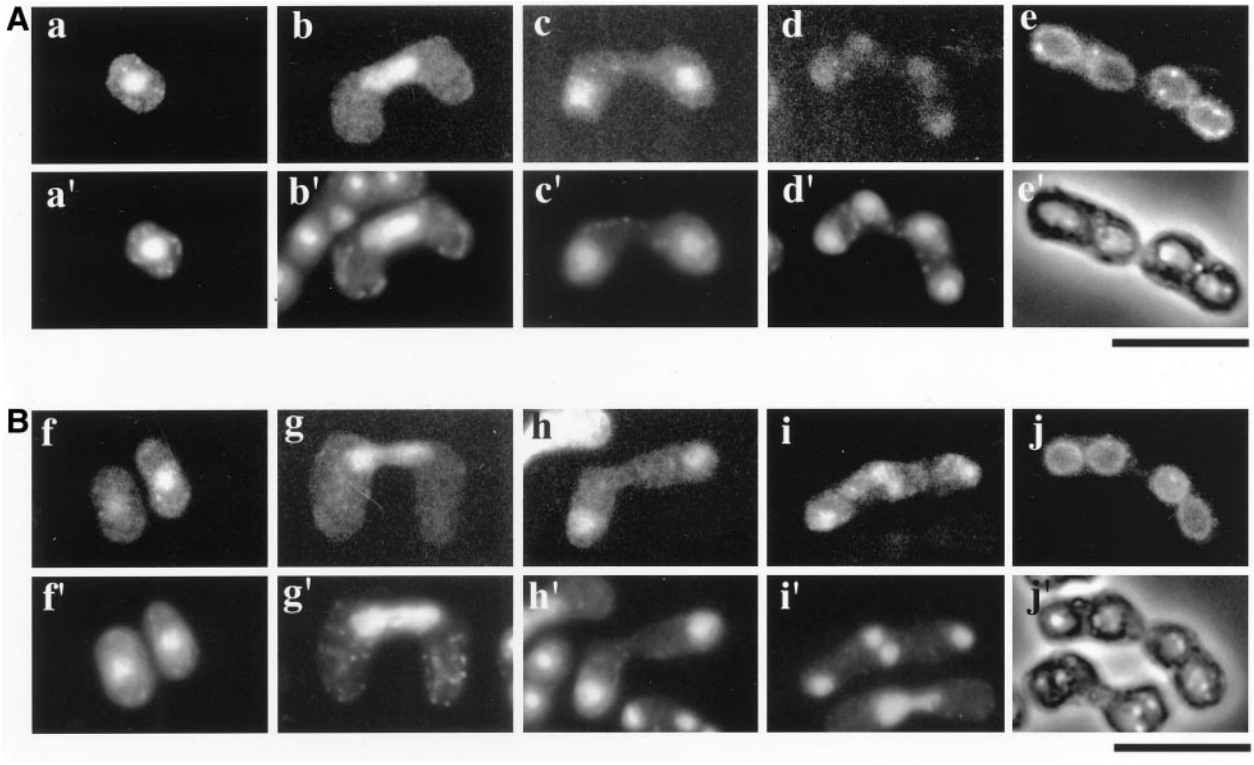

Figure 9. Localization of Spo20 during meiosis and sporulation. Homothallic haploid strain YN8-WH cells harboring integrated *spo20*$^{+}$-HA (A) and TN9 carrying pAL(*spo20*^{G275D}-HA) (B) were cultured in SSL-N to induce meiosis. Fixed cells were observed at different stages of meiosis using anti-HA antibody (a–j) and DAPI (a′–d′, f′–i′), as well as observed by phase-contrast microscopy (e′ and j′). a, a′, f, and f′, cells arrested on nitrogen starvation; b, b′, g, and g′, cells in prophase I; c, c′, h, and h′, cells in meiosis I; d, d′, i, and i′, cells in meiosis II; e, e′, j, and j′, sporulated cells. Bars, 10 μm.

Spo20 and Formation of Forespore Membrane

We next examined in greater detail how the *spo20-KC104* mutation impairs the sporulation process. During meiosis II, SPBs structurally change from a compact dot to a crescent (Hagan and Yanagida, 1995). The latter morphology corresponds to enlargement of SPBs into structures having multilayered outer plaques (Hirata and Tanaka, 1982; Tanaka and Hirata, 1982). This SPB modification is presumed to be indispensable for spore formation (Hirata and Shimoda, 1992; Ikemoto *et al.*, 2000). In *spo20* cells, crescent-shaped SPBs are formed as in wild-type cells (Figure 11A), suggesting that the sporulation defect of the *spo20* mutant is not due to a defect in the structural modification of SPB during meiosis II.

Finally, we investigated the assembly of forespore membranes in *spo20* mutant cells. Forespore membranes were marked with Spo3-GFP. In wild-type cells, forespore membranes completely enclosed the haploid nuclei produced by meiotic second divisions (Figure 11B). By contrast, forespore membranes were abnormally assembled in *spo20* mutants (Figure 11, B and C). Only 10% of the zygotes contained four complete sets of nucleated prespores. Anucleate prespores were observed in some 30% of the zygotes, whereas 40% of

Figure 10. Spo20 is localized to forespore membranes in late meiosis. Colocalization of Spo3 and Spo20 in meiotic cells. Wild-type strain YN9-WH harboring chromosomally integrated *spo20*$^{+}$*-HA* was transformed with pAL(spo3-GFP). This strain was cultured in SSL-N to induce meiosis. After fixation, localization of Spo3 was visualized by GFP and that of Spo20 was detected by anti-HA antibody. Bar, 10 μm.

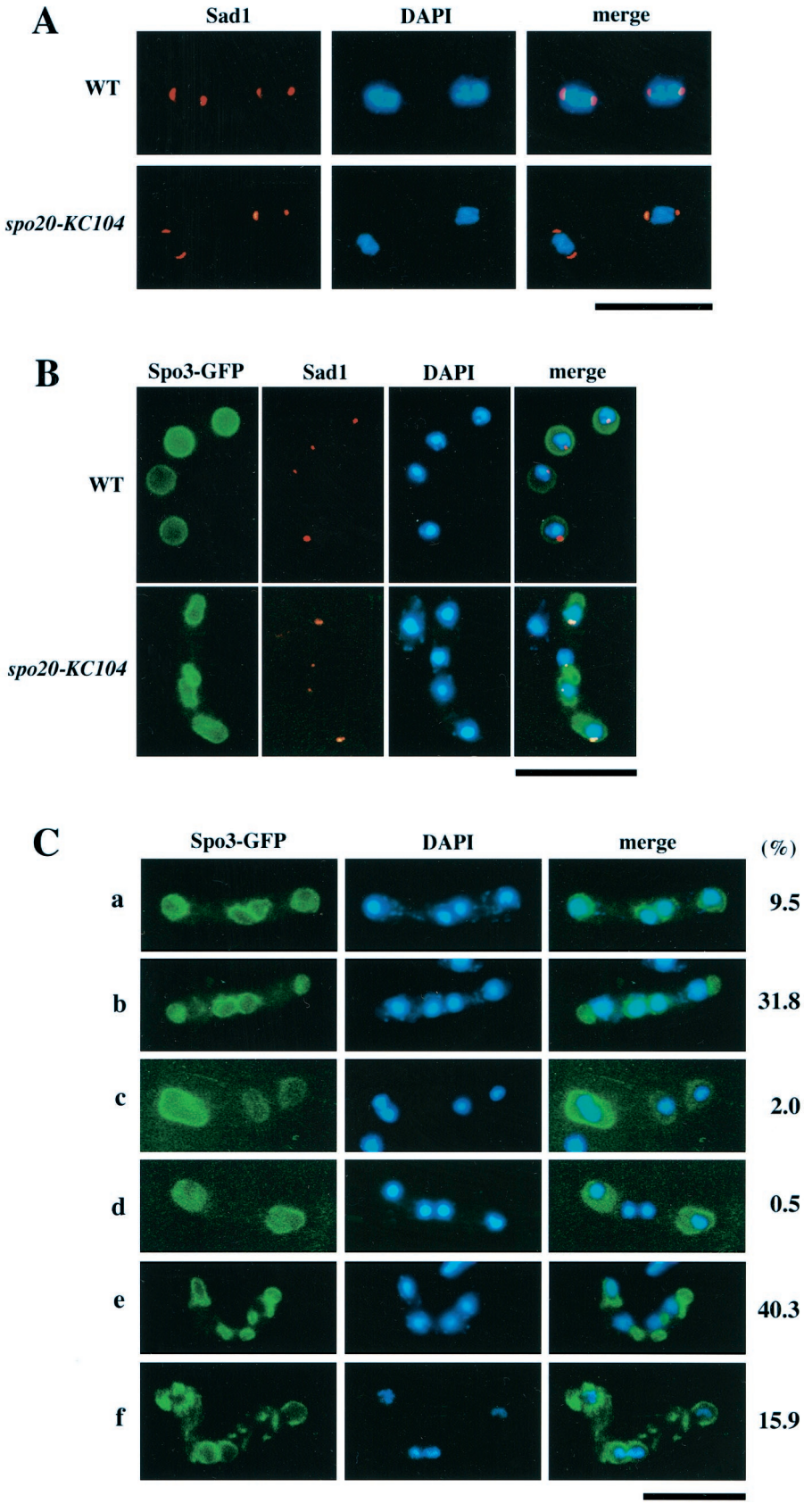

Figure 11. Abnormal sporulation in *spo20-KC104*. (A) The morphological change in SPBs from dot to crescent forms during meiosis II is normal in *spo20-KC104*. A wild-type strain (SI53) and a *spo20* mutant strain (YN11) were cultured in SSL-N sporulation medium and doubly stained with the anti-Sad1 antibody and DAPI. (B) Forespore membrane formation is abnormal in *spo20-KC104*. Wild-type (C766–1A) and *spo20* mutant (YN11) cells transformed with pAL(*spo3-GFP*) were cultured in SSL-N to induce meiosis. Fixed cells were examined using DAPI and GFP, as well as anti-Sad1 antibodies. (C) Assembly of forespore membranes and their enclosure of nuclei in *spo20-KC104* cells. *spo20* mutant (YN11) cells transformed with pAL(*spo3-GFP*) were cultured in SSL-N to induce meiosis. Forespore membranes and chromatin regions were visualized by GFP and DAPI, respectively. Stained cells were categorized into the following six classes: all four prespores enclose the nucleus (a); four prespores were formed but some of them do not enclose the nucleus (b); three prespores (c), two prespores (d), more than five prespores (e) were formed; forespore membranes were fragmented (f). Bars, 10 μm.

the zygotes contained more than five prespores. These findings confirm previous electron microscopy studies documenting formation of aberrant prespores in *spo20* mutants (Hirata and Shimoda, 1992). In conclusion, Spo20 appears either to be responsible for the normal construction of the forespore membrane or it coordinates forespore assembly with meiotic nuclear division.

DISCUSSION

We reported previously that the *spo20-KC104* mutation is sporulation specific (Kishida and Shimoda, 1986), and in the present study we show that *spo20*$^+$ is essential for forespore membrane assembly; however, we also document important vegetative functions for the *spo20*$^+$ gene product. We find that *spo20-KC104* is temperature sensitive for growth and that *spo20* null mutants are inviable. Our results also demonstrate that *spo20*$^+$ encodes a protein closely related to the budding yeast Sec14, which plays an essential role in protein transport from the yeast Golgi complex (Kearns *et al.*, 1998a). Indeed, heterologous complementation experiments indicate that Spo20 and Sec14 are functionally interchangeable in vivo. Moreover, Spo20 is Sec14-like in its biochemical properties as well, as indicated by our demonstration that Spo20 exhibits both PtdIns- and PtdCho-transfer activities in vitro. On that basis, Spo20 is a classical Sec14-type PITP and is not a member of the nonclassical Sfh-type PITP family of proteins that exhibit PtdIns-transfer activity only.

Subcellular localization experiments revealed that Spo20 localizes predominantly to cell poles during interphase and redistributes to both cell poles and medial septation sites during M-phase. In cell poles and the medial septation sites, membranes are actively remodeled by both biosynthetic and degradative mechanisms. These regions therefore may require the robust recruitment of membrane vesicles carrying secretory and membrane-associated proteins for cell surface growth and septation. Indeed, proteins required for septum formation and cell separation localize in the medial region of the cell as ring-like structures (Marks and Hyams, 1985; Marks *et al.*, 1986; Kitayama *et al.*, 1997; Katayama *et al.*, 1999; Toya *et al.*, 1999). Because localization of Spo20 and F-actin appears to be interdependent, Spo20 might effect the transport of secretory proteins to these growing regions in an F-actin-dependent manner. Mammalian PITPs likely regulate the fusion of secretory granules with the neuroendocrine plasma membrane by stimulating the synthesis of a dedicated pool of PtdIns-4,5-bisphosphate (Hay and Martin, 1993; Hay *et al.*, 1995). Spo20 might play an analogous role in fission yeast. Our demonstration that *spo20-KC104* mutants display defects in cell separation at the restrictive temperature is consistent with this view, and heterologous complementation experiments with a mutant Sec14p specifically defective in PtdIns-transfer activity are also suggestive (see below).

During meiosis and sporulation, the localization of Spo20 changes markedly. After the shift to nitrogen-starved medium, Spo20 translocates into the nucleus and accumulates there during sexual development; however, once sporulation commences, Spo20 redistributes to forespore membranes. The physiological significance of the nuclear localization of Spo20 after starvation is unclear, but it may facilitate an appropriate distribution of this protein to forespore membranes. These membranes are assembled in immediate proximity to meiotic nuclei.

The *spo20-KC104* mutant is temperature sensitive for growth yet exhibits a sporulation-defective phenotype at temperatures permissive for proliferation. Because Spo20^{G275D} resembles wild-type Spo20 in terms of abundance and subcellular localization, it is unlikely that sporulation defects result from the instability or mislocalization of the mutant protein during sporulation. Perhaps, Spo20 plays different roles in sporulating cells than in vegetative cells. This possibility is supported by our demonstration that the subcellular distribution of Spo20-HA in sporulating cells is different from its distribution in vegetative cells. A second possibility is that the threshold activity level of Spo20 required for sporulation is higher than that required for vegetative growth. We presently do not favor the latter model because expression of the PtdIns-transfer-deficient Sec14p^{K66,239A} protein in *spo20* mutants fully complements the sporulation defect but fails to complement the temperature sensitivity for vegetative growth. Those data suggest that although Spo20 PtdIns-transfer activity might be dispensable for sporulation in fission yeast, this activity is critical for at least one of the essential vegetative functions of Spo20. Given that Sec14^{K66,239A} is functional in promoting the Golgi secretory function in budding yeast (Phillips *et al.*, 1999) and that it retains the ability to down-regulate PtdCho synthesis via the CDP–choline pathway in *S. cerevisiae* (McGee *et al.*, 1994; Skinner *et al.*, 1995; Phillips *et al.*, 1999), we anticipate that Golgi function will not be defective in *spo20* mutants that express Sec14^{K66,239A}. Rather, we speculate that the septation function of Spo20 might require PtdIns-transfer activity. This hypothesis clarifies experimental predictions that are presently under investigation.

How might sporulating cells use Spo20 PtdCho transfer activity? Forespore membrane formation in *S. cerevisiae* requires *SPO14* (*ScSPO14*), the PLD structural gene (Wang *et al.*, 1994; Ella *et al.*, 1996; Waksman *et al.*, 1996; Rose *et al.*, 1995). Interestingly, ScSpo14 is initially distributed throughout the cell, is translocated to the SPB after the first meiotic division, and is ultimately localized to forespore membranes at meiosis II (Rudge *et al.*, 1998). This regulated redistribution of ScSpo14 during sporulation resembles the developmentally regulated redistribution that we document for Spo20. It is tempting to speculate that Spo20 facilitates PLD activation in fission yeast so that forespore membranes can be properly formed. The PtdCho-transfer activity of Spo20 might facilitate PLD activity by presenting PtdCho to the enzyme for efficient hydrolysis. This model demands that PLD activity is also required for forespore membrane biogenesis in fission yeast, and we have identified an ORF encoding a PLD-like protein in the fission yeast genome database (The Sanger Center, Cambridge, UK). The relationship between Spo20 function and activity of the PLD homologue is now under investigation. Nevertheless, this hypothesis differs from the developing picture in budding yeast, where the nonclassical Sfh proteins are required for optimal activation of PLD, at least in vegetative cells (Li *et al.* 2000). In that case, the Sfh proteins likely stimulate PLD activity by facilitating phosphoinositide biosynthesis (Li *et al.*, 2000).

Structural modification of SPB is a prerequisite to the assembly of forespore membranes (Hirata and Shimoda, 1992; Ikemoto *et al.*, 2000). We find that the SPB is modified

in *spo20* mutants, but many abnormal forespore membranes are assembled and mature spores fail to form. Most asci in *spo20* mutants contain one to four immature prespores bounded by forespore membranes. It may be of significance that some prespores in the *spo20* asci fail to engulf daughter nuclei, suggesting that Spo20 helps coordinate forespore membrane assembly with meiotic nuclear division.

In summary, we report that a fission yeast PITP, Spo20, functions not only in the previously recognized regulation of Golgi secretory function, but also in completion of septation in vegetative cells. It also plays a critical role in the biogenesis of forespore membranes when fission yeast effect a developmental switch to the sporulation program. The present study with *S. pombe*, when taken together with previous work in *S. cerevisiae* (Neiman, 1998), amply demonstrates the functional interface between proteins that regulate vegetative secretory pathway function and membrane assembly processes that accompany sporulation. Continued analyses of this functional interface will aid in elucidation of molecular mechanisms for gametogenesis. Finally, the data further expand the repertoire of important cellular functions that are modulated by PITPs and provide additional evidence to indicate that PITPs represent fundamental intracellular regulatory molecules.

ACKNOWLEDGMENTS

We thank A. Nakano and coworkers of RIKEN for *sec14* strains and useful discussions, K. Tanaka of the University of Tokyo, S. Forsburg of the Salk Institute, and M. Kubo of Osaka City University for plasmids, K. Gull of the University of Manchester for the anti-α-tubulin antibody, TAT-1, and O. Niwa of Kazusa DNA Research Institute for affinity-purified antibodies against Sad1. We also thank K. Takegawa and N. Tanaka (Kagawa University), M. Yamamoto and M. Toya (University of Tokyo), S. Kagiwada (Nara Women's University), and K. Hosaka (Gunma University) for their useful discussions. The present study was partly supported by Grants-in-Aid for Scientific Research on Priority Areas from the Ministry of Education, Science, Sports and Culture of Japan to C.S. and Saneyoshi Scholarship Foundation to T.N. S.R. and V.A.B. were supported by grant GM44530 from the National Institutes of Health.

REFERENCES

Aitken, J.F., van Heusden, G.P.H., Temkin, M., and Dowhan, W. (1990). The gene encoding the phosphatidylinositol transfer protein is essential for cell growth. J. Biol. Chem. *265*, 4711–4717.

Bankaitis, V.A., Aitken, J.R., Cleves, A.E., and Dowhan, W. (1990). An essential role for a phospholipid transfer protein in yeast Golgi function. Nature *347*, 561–562.

Bankaitis, V.A., Malehorn, D.E., Emr, S.D., and Greene, R. (1989). The *Saccharomyces cerevisiae SEC14* gene encodes a cytosolic factor that is required for transport of secretory proteins from the yeast Golgi complex. J. Cell. Biol. *108*, 1271–1281.

Beckers, D.M., Fikes, J.D., and Guarente, L. (1991). A cDNA encoding a human CCAAT-binding protein cloned by functional complementation in yeast. Proc. Natl. Acad. Sci. USA *88*, 1968–1972.

Bresch, C., Muller, G., and Egel, R. (1968). Genes involved in meiosis and sporulation of a yeast. Mol. Gen. Genet. *102*, 301–306.

Byers, B. (1981). Cytology of the yeast life cycle. In: The Molecular Biology of the Yeast *Saccharomyces cerevisiae*: Life Cycle and Inheritance, ed. J.N. Strathern, J.N., E.W. Jones, and J.R. Broach, J. R.), New York: Cold Spring Harbor Laboratory, 59–96.

Cleves, A.E., McGee, T.P., Whitters, E.A., Champion, K.M., Aitken, J.R., Dowhan, W., Goebl, M., and Bankaitis, V.A. (1991). Mutations in the CDP-choline pathway for phospholipid biosynthesis bypass the requirement for an essential phospholipid transfer protein. Cell *64*, 789–800.

Cleves, A.E., Novick, P.J., and Bankaitis, V.A. (1989). Mutations in the *SAC1* gene suppress defects in yeast Golgi and yeast actin function. J. Cell Biol. *109*, 2939–2950.

Egel, R. (1971). Physiological aspects of conjugation in fission yeast. Planta (Berl) *98*, 89–96.

Egel, R. (1989). Mating-type genes, meiosis and sporulation. In: Molecular Biology of the Fission Yeast, ed. A. Nasim, P. Young, and B.F. Johnson), San Diego, Academic Press, 31–73.

Egel, R., and Egel-Mitani, M. (1974). Premeiotic DNA synthesis in fission yeast. Exp. Cell Res. *88*, 127–134.

Ella, K.M., Dolan, J.W., Qi, C., and Meier, K.E. (1996). Characterization of *Saccharomyces cerevisiae* deficient in expression of phospholipase D. Biochem. J. *314*, 15–19.

Forsburg, S.L., and Sherman, D.A. (1997). General purpose tagging vectors for fission yeast. Gene *191*, 191–195.

Grimm, C., Kohli, J., Murray, J., and Maundrell, K. (1988). Genetic engineering of *Schizosaccharomyces pombe*: a system for gene disruption and replacement using the *ura4* gene as a selectable marker. Mol. Gen. Genet. *215*, 81–86.

Gutz, H., Heslot, H., Leupold, U., and Loprieno, N. (1974). *Schizosaccharomyces pombe*. In: Handbook of Genetics 1, New York: Plenum Press, 395–446.

Hagan, I., and Yanagida, M. (1995). The product of the spindle formation gene $sad1^{+}$ associates with the fission yeast spindle pole body and is essential for viability. J. Cell Biol. *129*, 1033–1047.

Hagan, I.M., and Hyams, J.S. (1988). The use of cell division cycle mutants to investigate the control of microtubule distribution in the fission yeast *Schizosaccharomyces pombe*. J. Cell Sci. *89*, 343–357.

Hay, J.C., Fissette, P.L., Jenkins, G.H., Fukami, K., Takenawa, T., Anderson, R.A., and Martin, T.F.J. (1995). ATP-dependent inositide phosphorylation required for Ca^{2+}-activeted secretion. Nature *374*, 173–177.

Hay, J.C., and Martin, T.F.J. (1993). Phosphatidylinositol transfer protein is required for ATP-dependent priming of Ca^{2+}-activated secretion. Nature *366*, 572–575.

Hirata, A., and Shimoda, C. (1992). Electron microscopic examination of sporulation-deficient mutants of the fission yeast *Schizosaccharomyces pombe*. Arch. Microbiol. *158*, 249–255.

Hirata, A., and Tanaka, K. (1982). Nuclear behavior during conjugation and meiosis in the fission yeast *Schizosaccharomyces pombe*. J. Gen. Appl. Microbiol. *28*, 263–274.

Ikemoto, S., Nakamura, T., Kubo, M., and Shimoda, C. (2000). *S. pombe* sporulation-specific coiled-coil protein Spo15p is localized to the spindle pole body and essential for its modification. J. Cell Sci. *113*, 545–554.

Ito, H., Fukuda, Y., Murata, K., and Kimura, A. (1983). Transformation of intact yeast cells treated with alkaline cations. J. Bacteriol. *153*, 163–168.

Jensen, R., Sprague, G.F., Jr., and Herskowitz, I. (1983). Regulation of yeast mating-type interconversion: feedback control of HO gene expression by the mating-type locus. Proc. Natl. Acad. Sci. USA *80*, 3035–3039.

Katayama, S., Hirata, D., Arellano, M., Perez, P., and Toda, T. (1999). Fission yeast alpha-glucan synthase Mok1 requires the actin cytoskeleton to localize the sites of growth and plays an essential role

in cell morphogenesis downstream of protein kinase C function. J. Cell Biol. *144*, 1173–1186.

Kearns, B.G., Alb, J.G., Jr., and Bankaitis, V.A. (1998a). Phosphatidylinositol transfer proteins: the long and winding road to physiological function. Trends Cell. Biol. *8*, 276–282.

Kearns, M.A., Monks, D.E., Fang, M., Rivas, M.P., Courtney, P.D., Chen, J., Prestwich, G.D., Theibert, A.B., Dewey, R.E., and Bankaitis, V.A. (1998b). Novel developmentally regulated phosphoinositide binding proteins from soybean whose expression bypasses the requirement for an essential phosphatidylinositol transfer protein in yeast. EMBO J. *17*, 4004–4017.

Kishida, M., Hirata, A., and Shimoda, C. (1990). A cold-sensitive *spo14* mutant affecting ascospore. Formation in the fission yeast *Shizosaccharomyces pombe*. Plant Cell. Physiol. *31*, 433–437.

Kishida, M., and Shimoda, C. (1986). Genetic mapping of eleven spo genes essential for ascospore formation in the fission yeast *Schizosaccharomyces pombe*. Curr. Genet. *10*, 443–447.

Kitayama, C., Sugimoto, A., and Yamamoto, M. (1997). Type II myosin heavy chain encoded by the myo2 gene composes the contractile ring during cytokinesis in *Schizosaccharomyces pombe*. J. Cell Biol. *137*, 1309–1319.

Li, X., Routt, S., Xie, Z., Cui, X., Fang, M., Kearns, M.A., Bard, M., Kirsch, D., and Bankaitis, V.A. (2000). Identification of a novel family of nonclassical yeast PITPs whose function modulates activation of phospholipase D and Sec14p-independent cell growth. Mol. Biol. Cell *11*, 1989–2005.

Losson, R., and Lacroute, F. (1983). Plasmids carrying the yeast OMP decarboxylase structural and regulatory genes: transcription regulation in a foreign environment. Cell *32*, 371–377.

Marks, J., Hagan, I.M., and Hyams, J.S. (1986). Growth polarity and cytokinesis in fission yeast: the role of the cytoskeleton. J. Cell Sci. Suppl. *5*, 229–241.

Marks, J., and Hyams, J. (1985). Localization of F-actin through the cell division cycle of *Schizosaccharomyces pombe*. Eur. J. Cell Biol. *39*, 27–32.

Masai, H., Miyake, T., and Arai, K. (1995). *hsk1*$^+$, a *Schizosaccharomyces pombe* gene related to *Saccharomyces cerevisiae* CDC7, is required for chromosomal replication. EMBO J. *14*, 3094–3104.

Maundrell, K. (1993). Thiamine-repressible expression vectors pREP and pRIP for fission yeast. Gene *123*, 127–130.

McGee, T.P., Skinner, H.B., and Bankaitis, V.A. (1994). Functional redundancy of CDP-ethanolamine and CDP-choline pathway enzymes in phospholipid biosynthesis: ethanolamine-dependent effects on steady-state membrane phospholipid composition in *Saccharomyces cerevisiae*. J. Bacteriol. *176*, 6861–6868.

Mitchison, J.M., and Nurse, P. (1985). Growth in cell length in the fission yeast *Schizosaccharomyces pombe*. J. Cell Sci. *75*, 357–376.

Moreno, S., Klar, A., and Nurse, P. (1990). Molecular genetic analysis of fission yeast *Schizosaccharomyces pombe*. Methods Enzymol. *194*, 793–823.

Neiman, A.M. (1998). Prospore membrane formation defines a developmentally regulated branch of the secretory pathway in yeast. J. Cell Biol. *140*, 29–37.

Novick, P., Field, C., and Schekman, R. (1980). Identification of 23 complementation groups required for post-translational events in the yeast secretory pathway. Cell *21*, 205–215.

Phillips, S.E., Sha, B., Topalof, L., Xie, Z., Alb, J.G., Klenchin, V.A., Swigart, P., Cockcroft, S., Martin, T.F., Luo, M., and Bankaitis, V.A. (1999). Yeast Sec14p deficient in phosphatidylinositol transfer activity is functional in vivo. Mol. Cell. *4*, 187–97.

Rose, K., Rudge, S.A., Frohman, M.A., Morris, A.J., and Engebrecht, J. (1995). Phospholipase D signaling is essential for meiosis. Proc. Natl. Acad. Sci. USA *92*, 12151–12155.

Rudge, S.A., Morris, A.J., and Engebrecht, J. (1998). Relocalization of phospholipase D activity mediates membrane formation during meiosis. J. Cell Biol. *140*, 81–90.

Sha, B., Phillips, S.E., Bankaitis, V.A., and Luo, M. (1998). Crystal structure of the *Saccharomyces cerevisiae* phosphatidylinositol-transfer protein. Nature *391*, 506–510.

Sherman, F., Fink, G.R., and Hicks, J.B. (1983). Methods in Yeast Genetics, Cold Spring Harbor, NY: Cold Spring Laboratory Press.

Skinner, H.B., Alb, J.G., Jr., Whitters, E.A., Helmkamp, G.M., Jr., and Bankaitis, V.A. (1993). Phospholipid transfer activity is relevant to but not sufficient for the essential function of the yeast *SEC14* gene product. EMBO J.*12*, 4775–4784.

Skinner, H.B., McGee, T.P., McMaster, C.R., Fry, M.R., Bell, R.M., and Bankaitis, V.A. (1995). The *Saccharomyces cerevisiae* phosphatidylinositol-transfer protein effects a ligand-dependent inhibition of choline-phosphate cytidylyltransferase activity. Proc. Natl. Acad. Sci. USA *92*, 112–116.

Tanaka, K., and Hirata, A. (1982). Ascospore development in the fission yeasts *Schizosaccharomyces pombe* and *S. japonicus*. J. Cell Sci. *56*, 263–279.

Tanaka, K., Yonekawa, T., Kawasaki, Y., Kai, M., Furuya, K., Iwasaki, M., Murakami, H., Yanagida, M., and Okayama, H. (2000). Fission yeast Eso1p is required for establishing sister chromatid cohesion during S phase. Mol. Cell. Biol. *20*, 3459–3469.

Thomas, P.S. (1980). Hybridization of denatured RNA and small DNA fragments transferred to nitrocellulose. Proc. Natl. Acad. Sci. USA *77*, 5201–5205.

Toya, M., Iino, Y., and Yamamoto, M. (1999). Fission yeast Pob1p, which is homologous to budding yeast Boi proteins and exhibits subcellular localization close to actin patches, is essential for cell elongation and separation. Mol. Biol. Cell *10*, 2745–2757.

Waksman, M., Eli, Y., Liscovitch, M., and Gerst, J.E. (1996). Identification and characterization of a gene encoding phospholipase D activity in yeast. J. Biol. Chem. *271*, 2361–2364.

Wang, X., Xu, L., and Zheng, L. (1994). Cloning and expression of phosphatidylcholine-hydrolyzing phospholipase D from Ricinus communis L. J. Biol. Chem. *269*, 20312–20317.

Woods, A., Sherwin, T., Sasse, R., MacRae, T.H., Baines, A.J., and Gull, K. (1989). Definition of individual components within the cytoskeleton of Trypanosoma brucei by a library of monoclonal antibodies. J. Cell Sci. *93*, 491–500.

Yamamoto, M., Imai, Y., and Watanabe, Y. (1997). Mating and sporulation in *Schizosaccharomyces pombe.* In: Molecular and Cellular Biology of the Yeast *Saccharomyces*, ed. J.R. Pringle, J.B. Broach, and E.W. Jones, New York: Cold Spring Harbor Laboratory Press, 1037–1106.

Yoo, B.Y., Calleja, G.B., and Johnson, B.F. (1973). Ultrastructural changes of the fission yeast (*Schizosaccharomyces pombe*) during ascospore formation. Arch. Mikrobiol. *91*, 1–10.